



# Predicting Microstructural Stability for Advanced FE Systems

**Youhai Wen, Jeffrey Hawk, David Alman**

ORD, NETL

**May 19-23, 2014**



U.S. DEPARTMENT OF  
**ENERGY** | National Energy  
Technology Laboratory

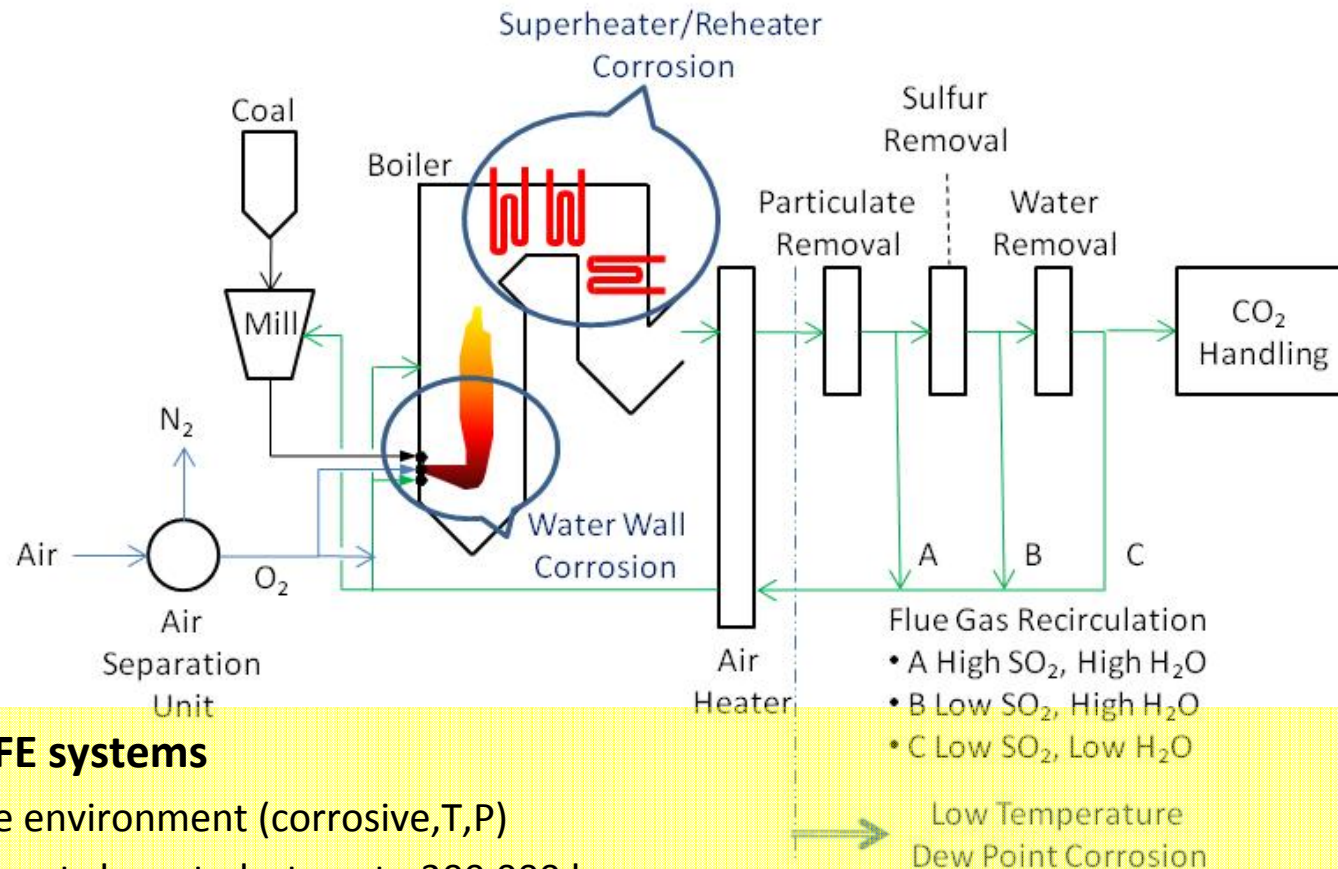
*2014 NETL Crosscutting Research Review Meeting*

# Acknowledgements

- **Strategic Center for Coal, NETL for supporting this ORD activity through the IPT Program.**
  - Susan Maley (Technology Manager)
  - Charles Miller (Project Monitor)
  - Vito Cedro (SCC)
  - Tianle Cheng (ORISE postdoc)
  - Nan Wang and Long-Qing Chen (Penn State)

*Disclaimer: "This report was prepared as an account of work sponsored by an agency of the United States Government. Neither the United States Government nor any agency thereof, nor any of their employees, makes any warranty, express or implied, or assumes any legal liability or responsibility for the accuracy, completeness, or usefulness of any information, apparatus, product, or process disclosed, or represents that its use would not infringe privately owned rights. Reference herein to any specific commercial product, process, or service by trade name, trademark, manufacturer, or otherwise does not necessarily constitute or imply its endorsement, recommendation, or favoring by the United States Government or any agency thereof. The views and opinions of authors expressed herein do not necessarily state or reflect those of the United States Government or any agency thereof."*

# NETL Strategies to Mitigate Materials Degradation under Harsh Service Conditions



## Advanced FE systems

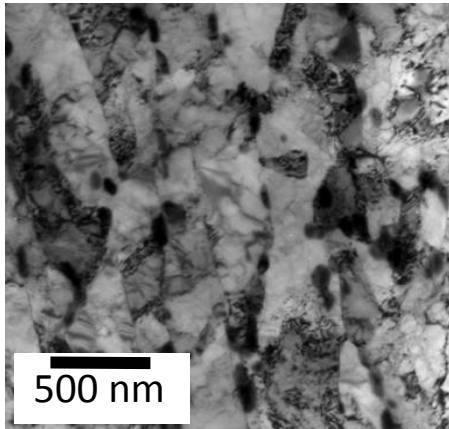
- Extreme environment (corrosive, T, P)
- Components have to last up to 300,000 hours
- *Lack of experience with alloy performance in these conditions*

***An integral computational and experimental approach to mitigate materials degradation***

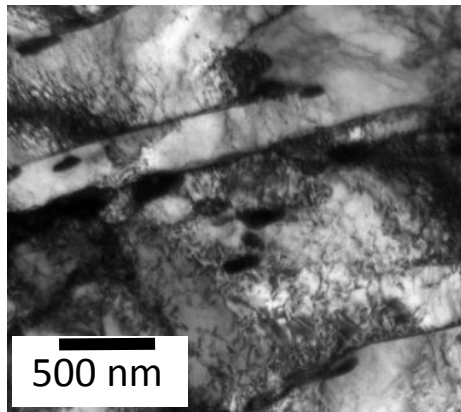
# Life Prediction: Microstructural Evolution

Subgrain, precipitate, and dislocation structure

As tempered

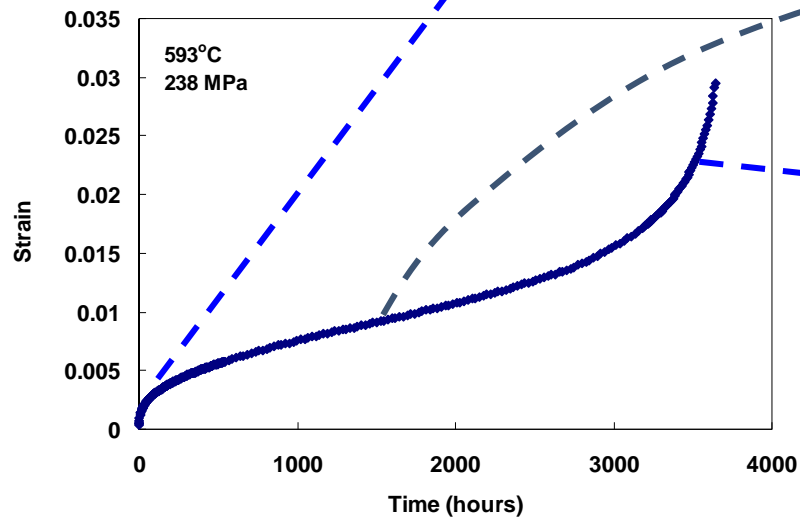
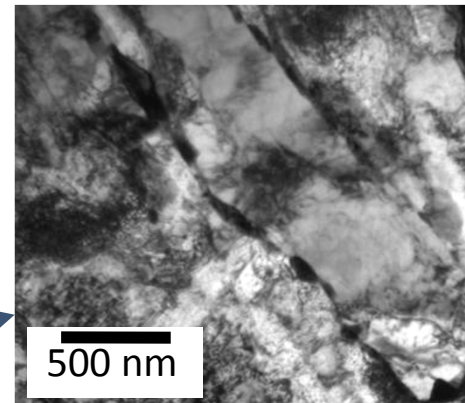


Primary – 100 h

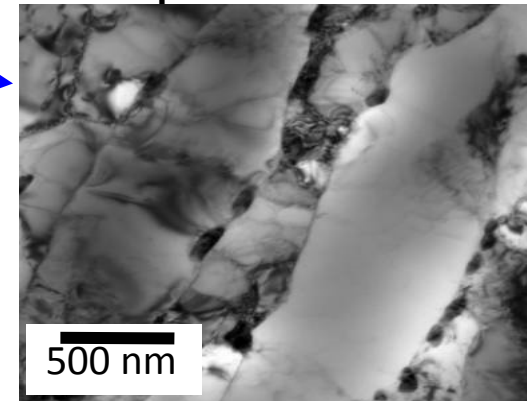


*Crept GAGE – 1100 °F*

Secondary – 1000 h



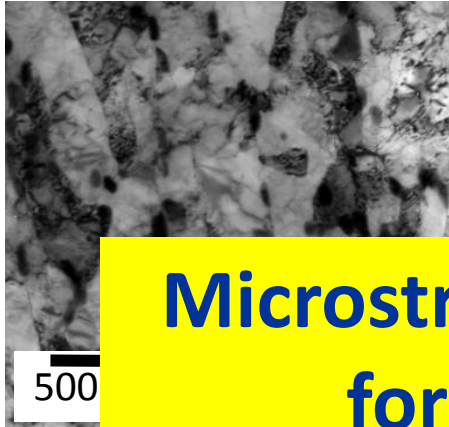
Rupture – 3000 h



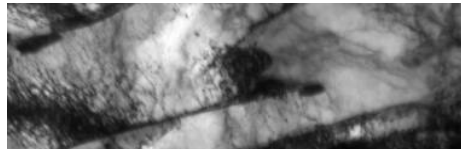
# Life Prediction: Microstructural Evolution

Subgrain, precipitate, and dislocation structure

As tempered



Primary – 100 h

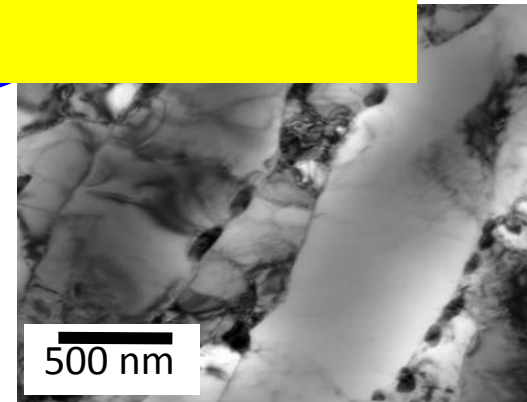
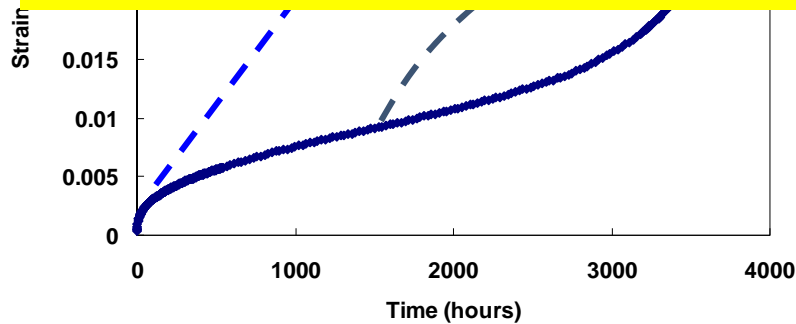


*Crept GAGE – 1100 °F*

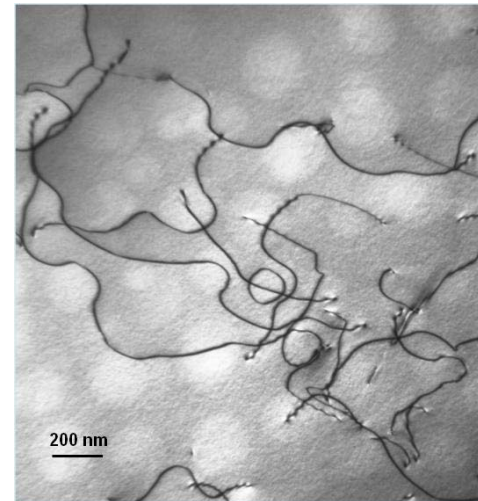
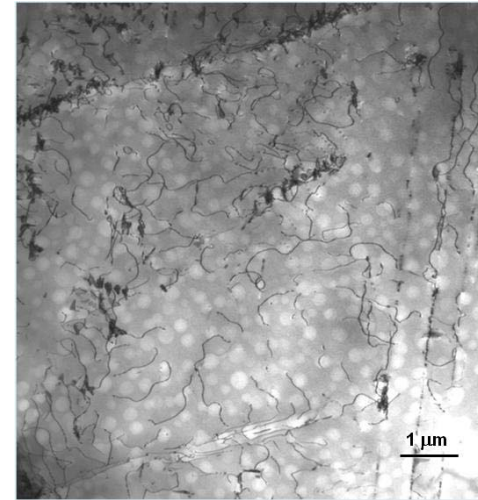
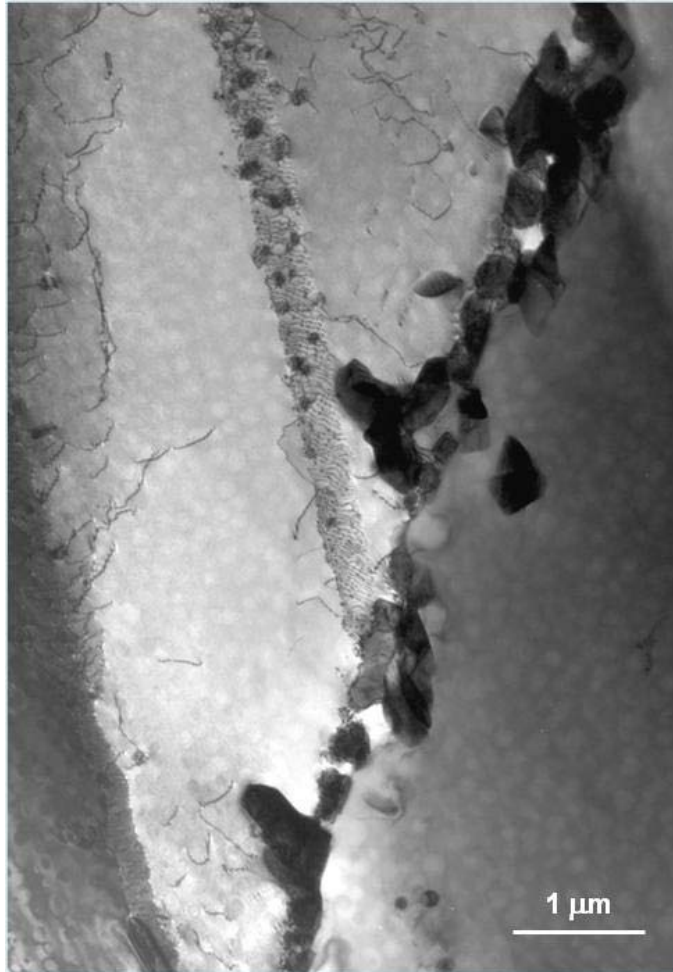
Secondary – 1000 h



**Microstructural evolution is inevitable for the high temperature FE environment, the only option left to extend the life of a material is to slow down this process**



Three most important things to slow down microstructure evolution:  
**Precipitates, precipitates, and precipitates!**

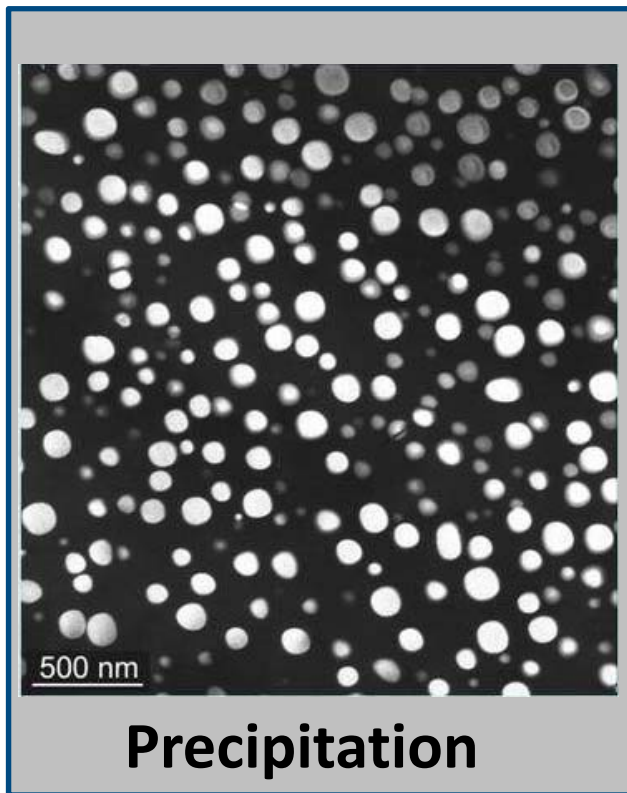


**Precipitates Pin Boundaries & Stabilize Structure as well as  
Hindering Dislocation Motion**

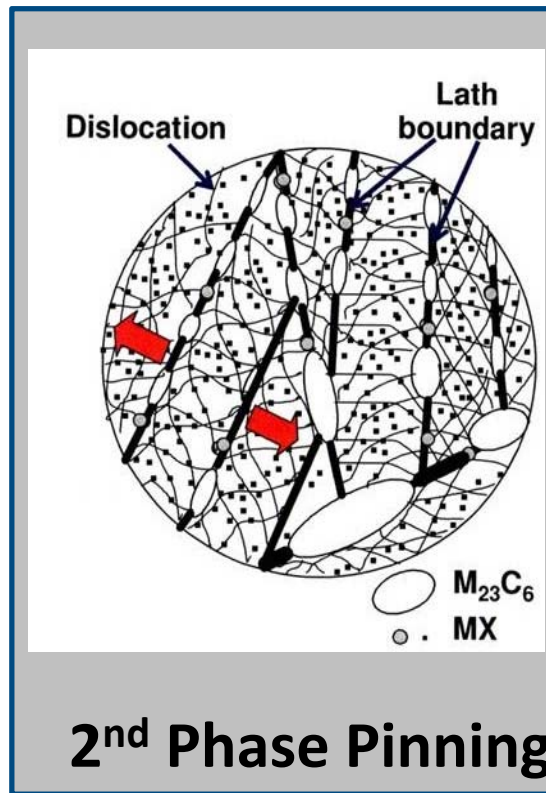


# NETL Microstructural Stability

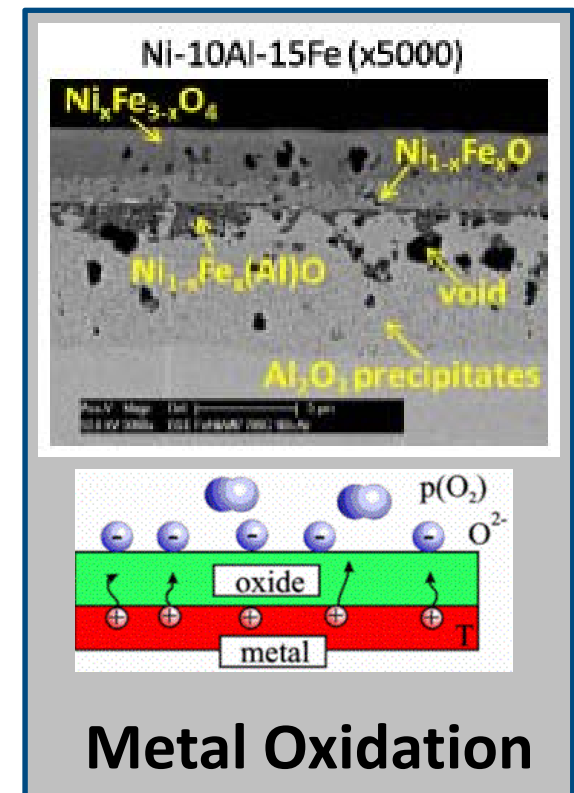
## Focused Areas of Modeling



Matrix Strength



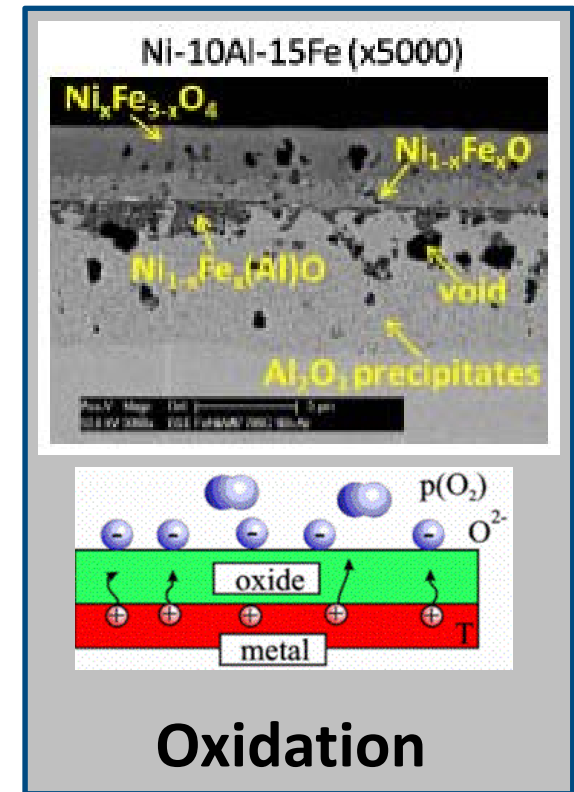
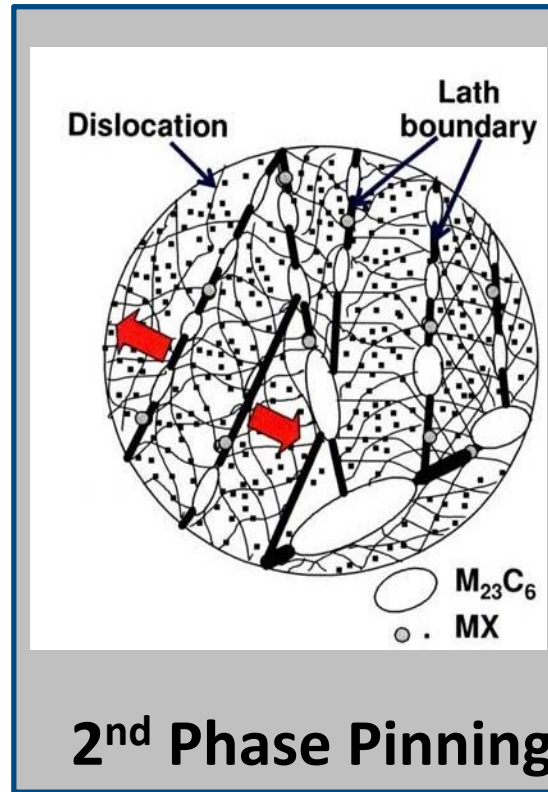
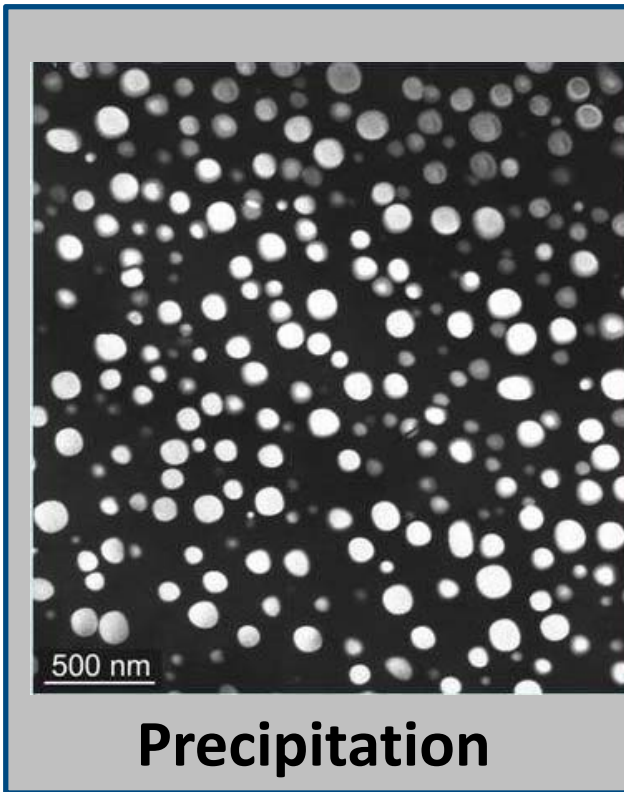
Grain Boundary Strength



Surface Attack

# NETL Microstructural Stability

## Focused Areas of Modeling

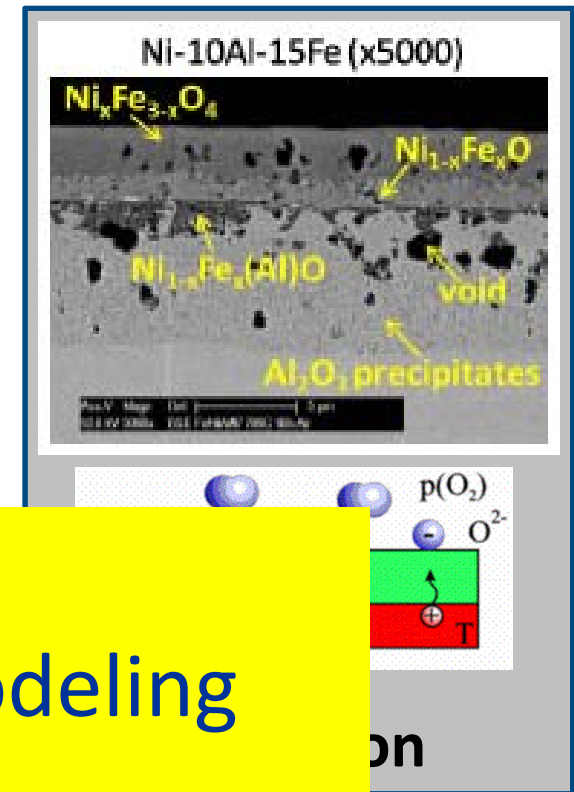
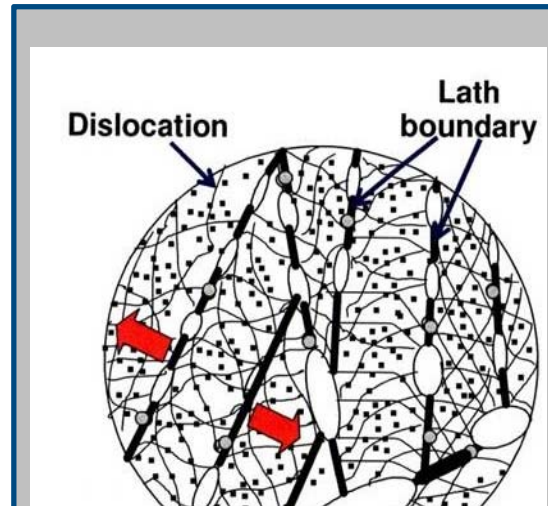
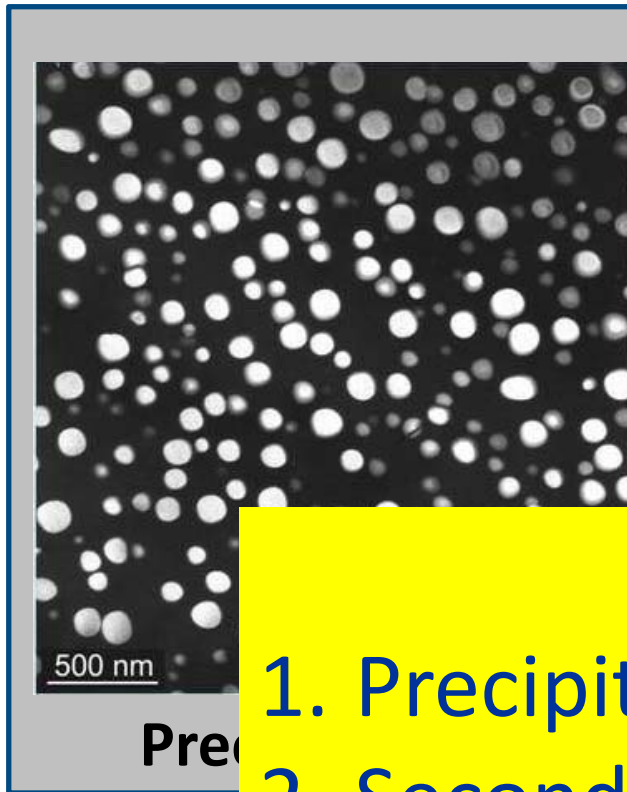


**IPT Task 5.4**  
**Microstructure Modeling**

**IPT Task 5.3**  
**Oxidation Modeling**

# NETL Microstructural Stability

## Focused Areas of Modeling

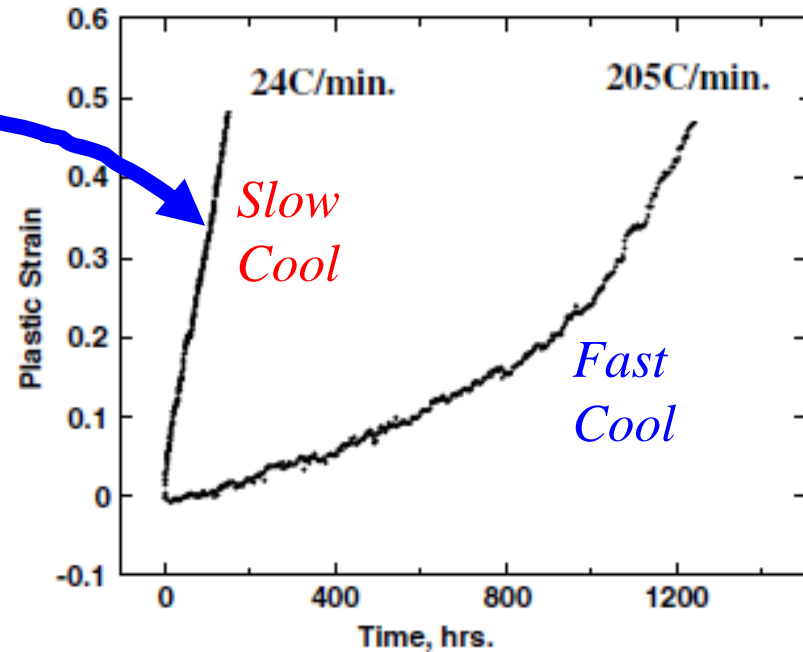
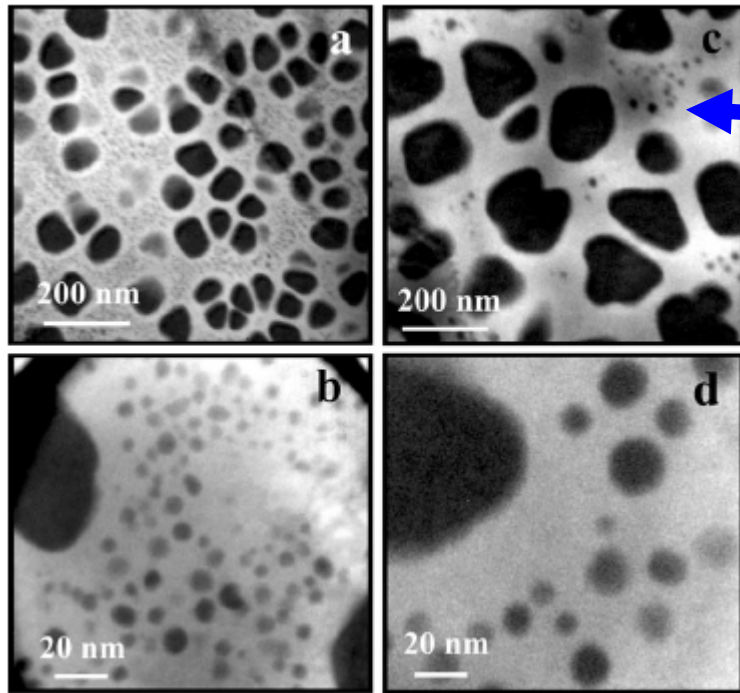


### Outline

1. Precipitation kinetics modeling
2. Second phase pinning
3. Oxidation kinetics modeling

# The Precipitation Modeling

205 C/min    24 C/min



Rene 88DT Disk Alloy

G.B.Viswanathan, et al Acta mater. 2005

## Microstructure and Performance

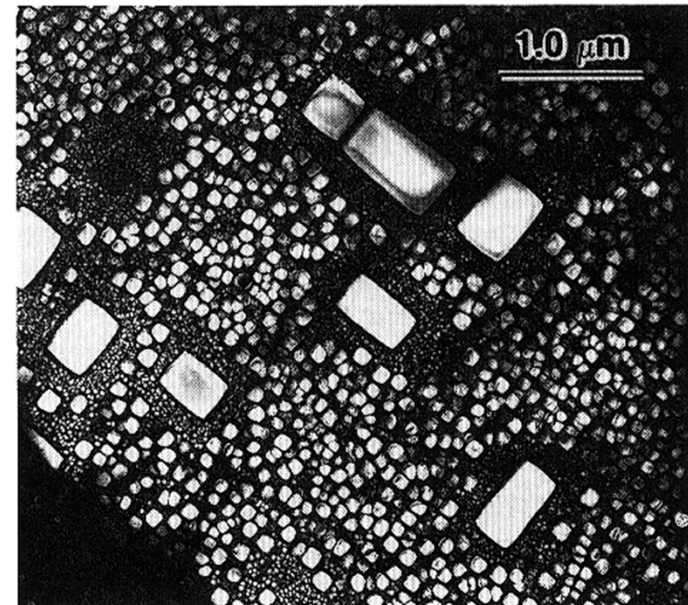
# The Precipitation Modeling

**Goal:** Develop an engineering tool that can predict precipitation process under representative thermomechanical processing and service conditions

## The Challenges

- High volume fraction of precipitates excluding any analytical solutions
- Complex thermal heat treating & thermo mechanical service condition
- Multi-component & multi-phase

Phase-field method has the potential



M.E. Gurtin and P.W. Voorhees.

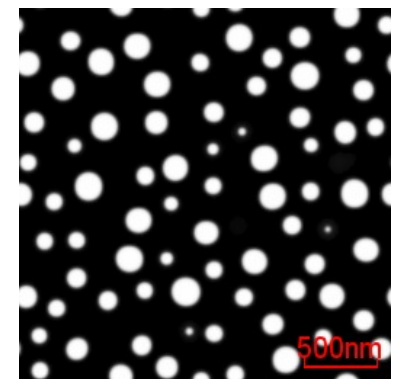
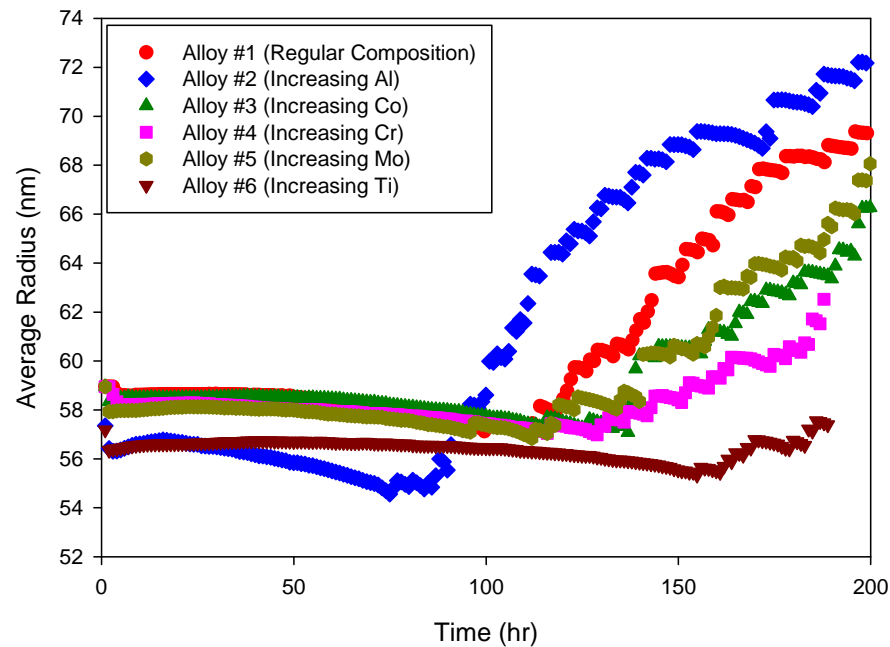
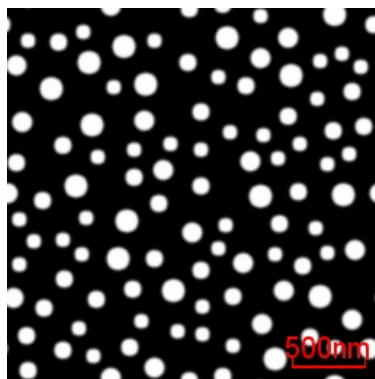
# NETL Multi-Component Phase-Field Precipitation Model

- **1D, 2D, and 3D capability**
- **Multi-Component: 7 components in present work**
- **Two phases:  $\gamma$  and  $\gamma'$  in Ni-base superalloys**
- **Direct link to CALPHAD Database: PanEngine from CompuTherm**

# Haynes 282 Precipitation Kinetics

Baseline alloy ↔

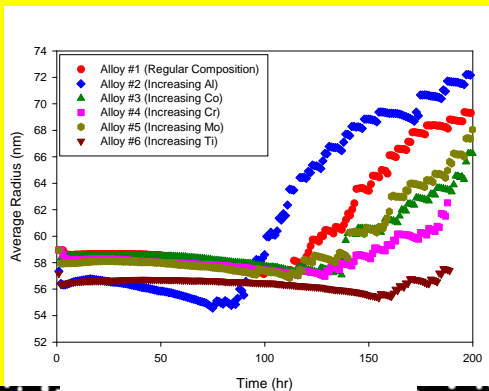
	Al	Co	Cr	Fe	Mo	Ti	Ni	Vol.%
<b>1</b>	1.5	10.0	20.0	1.5	8.5	2.1	Bal	18.86
<b>2</b>	<b>1.8</b>	10.0	20.0	1.5	8.5	2.1	Bal	21.08
<b>3</b>	1.5	<b>11.0</b>	20.0	1.5	8.5	2.1	Bal	18.91
<b>4</b>	1.5	10.0	<b>21.0</b>	1.5	8.5	2.1	Bal	18.97
<b>5</b>	1.5	10.0	20.0	1.5	<b>9.5</b>	2.1	Bal	19.05
<b>6</b>	1.5	10.0	20.0	1.5	8.5	<b>2.5</b>	Bal	21.62



Developing a Virtual Tool for Alloy Chemistry Screening

# Precipitation Kinetics Modeling Results

	Al	Co	Cr	Fe	Mo	Ti	Ni	Vol. %
1	1.5	10.0	20.0	1.5	8.5	2.1	Bal	18.86
2	1.8	10.0	20.0	1.5	8.5	2.1	Bal	21.08
3	1.5	11.0	20.0	1.5	8.5	2.1	Bal	18.91
4	1.5	10.0	21.0	1.5	8.5	2.1	Bal	18.97
5	1.5	10.0	20.0	1.5	9.5	2.1	Bal	19.05
6	1.5	10.0	20.0	1.5	8.5	2.5	Bal	21.62

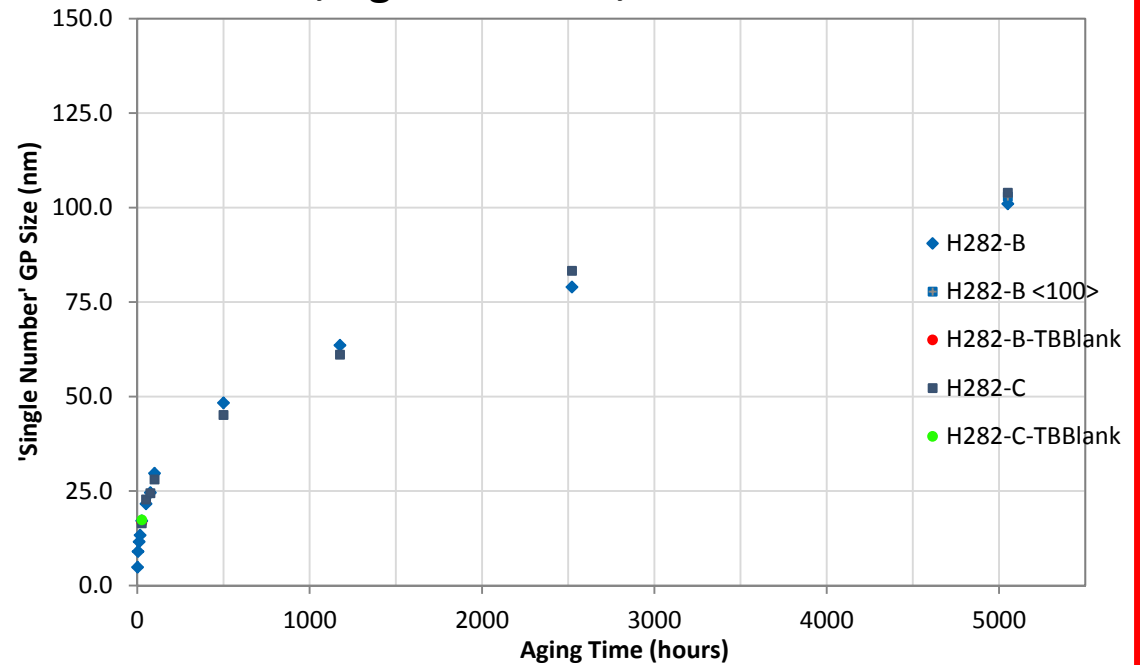


Alloy	Ni	Cr	Co	Mo	Ti	Al	Fe	Mn	Si	C	B ppm
Nominal	Bal	18.5-20.5	9-11	8-9	1.9-2.3	1.38-1.65	1.5*	0.3*	0.15*	0.04-0.08	30-50
H282-B	Bal	19.22	9.86	8.49	2.22	1.27		0.25	0.15	0.08	100
H282-C	Bal	19.19	9.85	8.50	1.94	1.54		0.25	0.14	0.08	100

H282B – Alloy # 6

H282C – Alloy 2

H282-B & -C, Aged at 760°C, Water Quenched

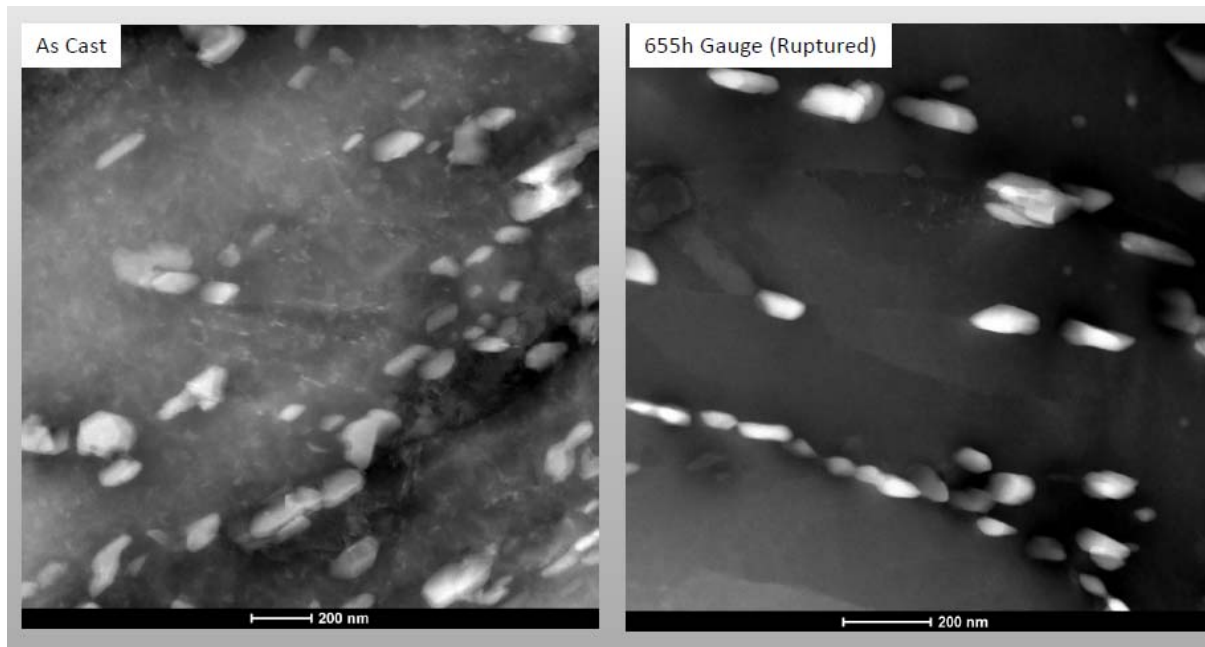


Verifying predictions, work in progress

# Summary of Precipitation Modeling

- **Developed a multicomponent Phase-Field model that can simulate precipitation kinetics in Ni-based commercial alloys**
- **Demonstrated that this model has the potential to be used for composition screening for a more stable precipitation microstructure**

# Second Phase Pinning Modeling

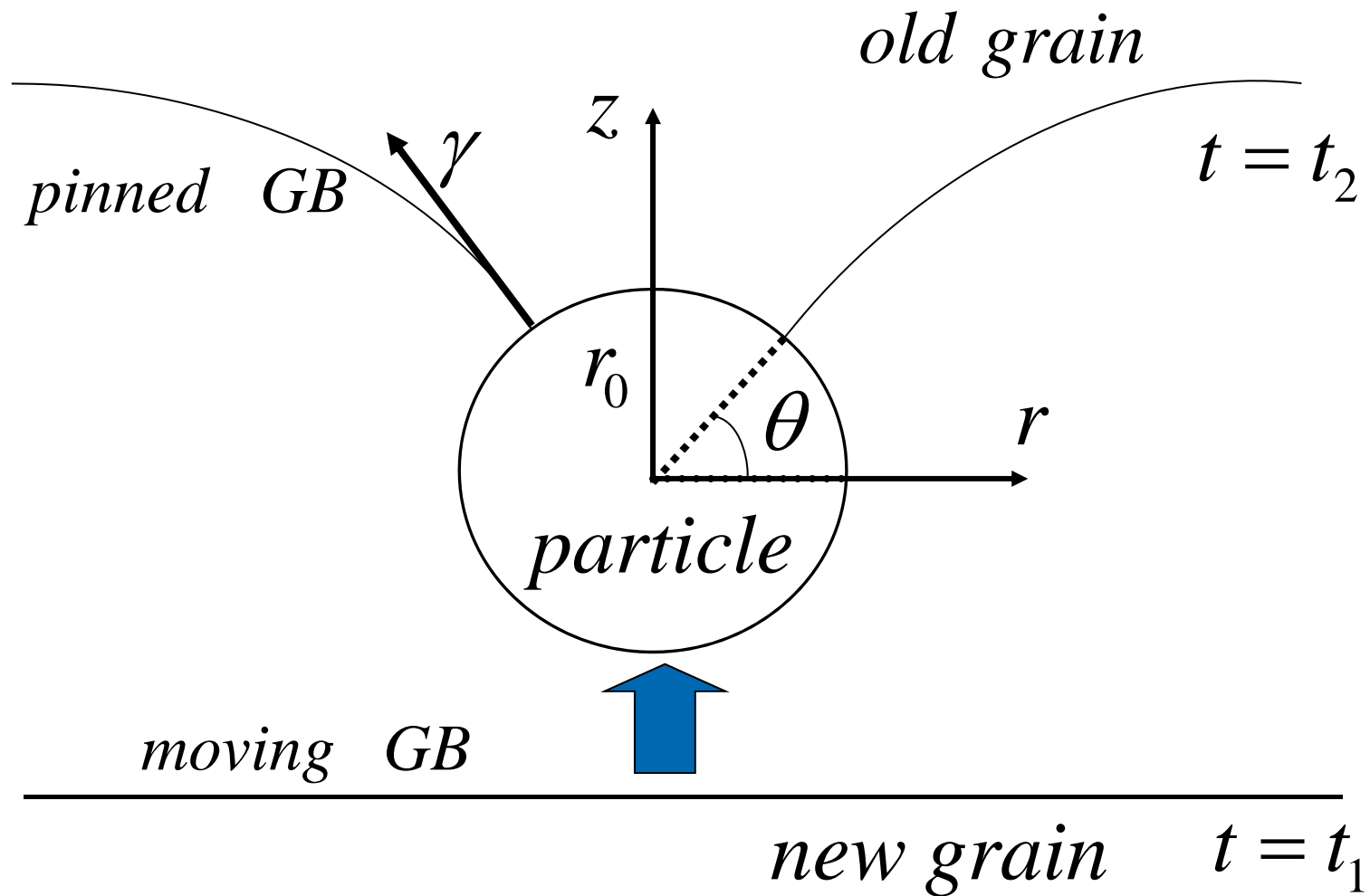


Courtesy of Mitsu Murayama at VirginiaTech

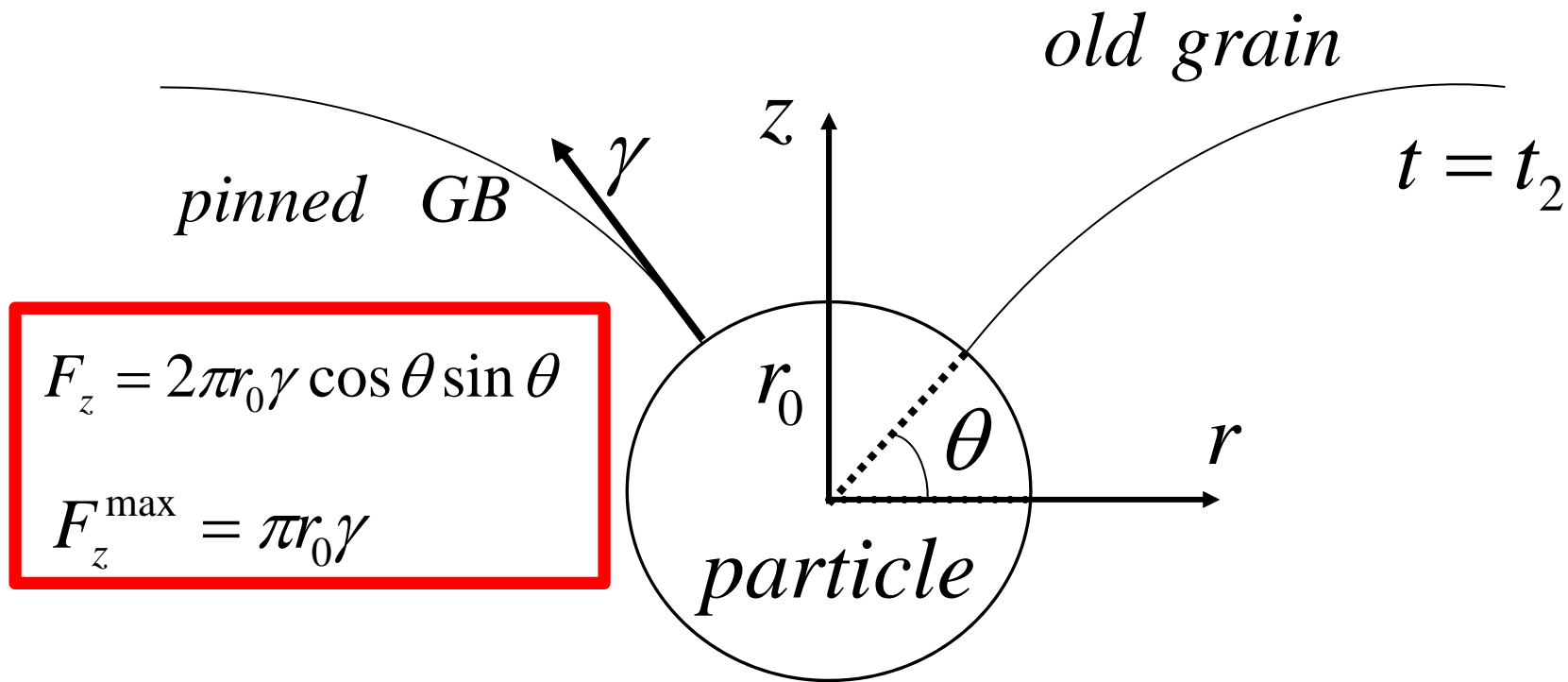
Carbide Precipitations in 9Cr Steel

**Second Phase Particles are not Spherical!**

# Particle Pinning Process



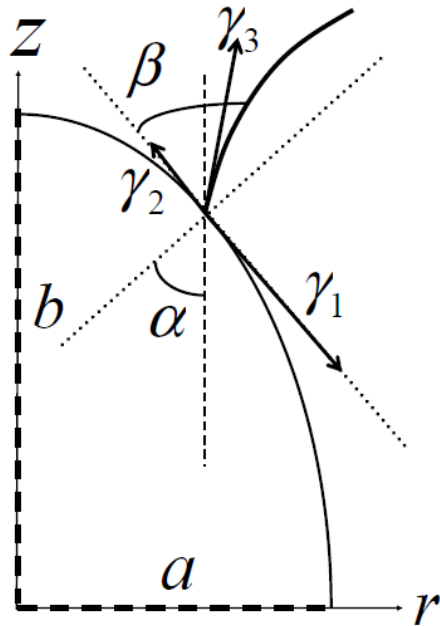
# Zenner Particle Pinning Theory



- Spherical second phase particle
- Incoherent interfaces

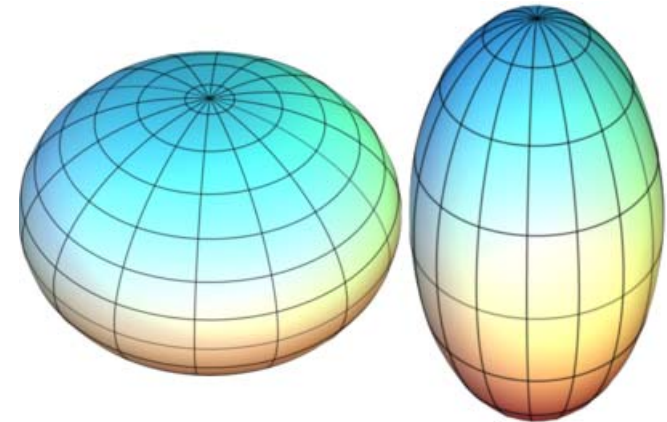
These two constraints are relaxed in this project

# New Theory and Validation for Ellipsoid Particles

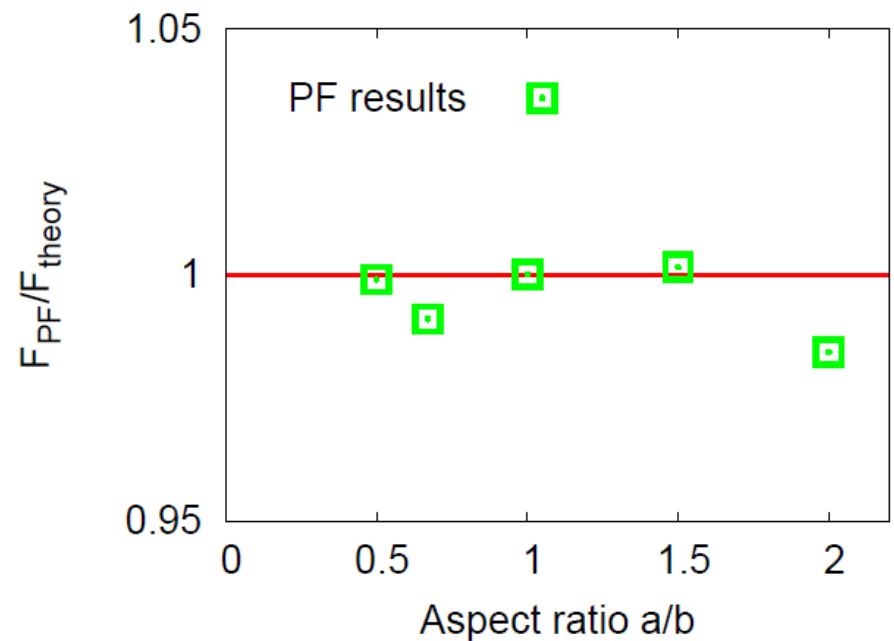


$$F_z = 2\pi\gamma_3 a \varepsilon \frac{\sin \alpha \cos[\alpha - (\pi/2 - \beta)]}{\sqrt{\cos^2 \alpha (1 - \varepsilon^2) + \varepsilon^2}}$$

$$\cos \beta = \frac{\gamma_1 - \gamma_2}{\gamma_3}$$

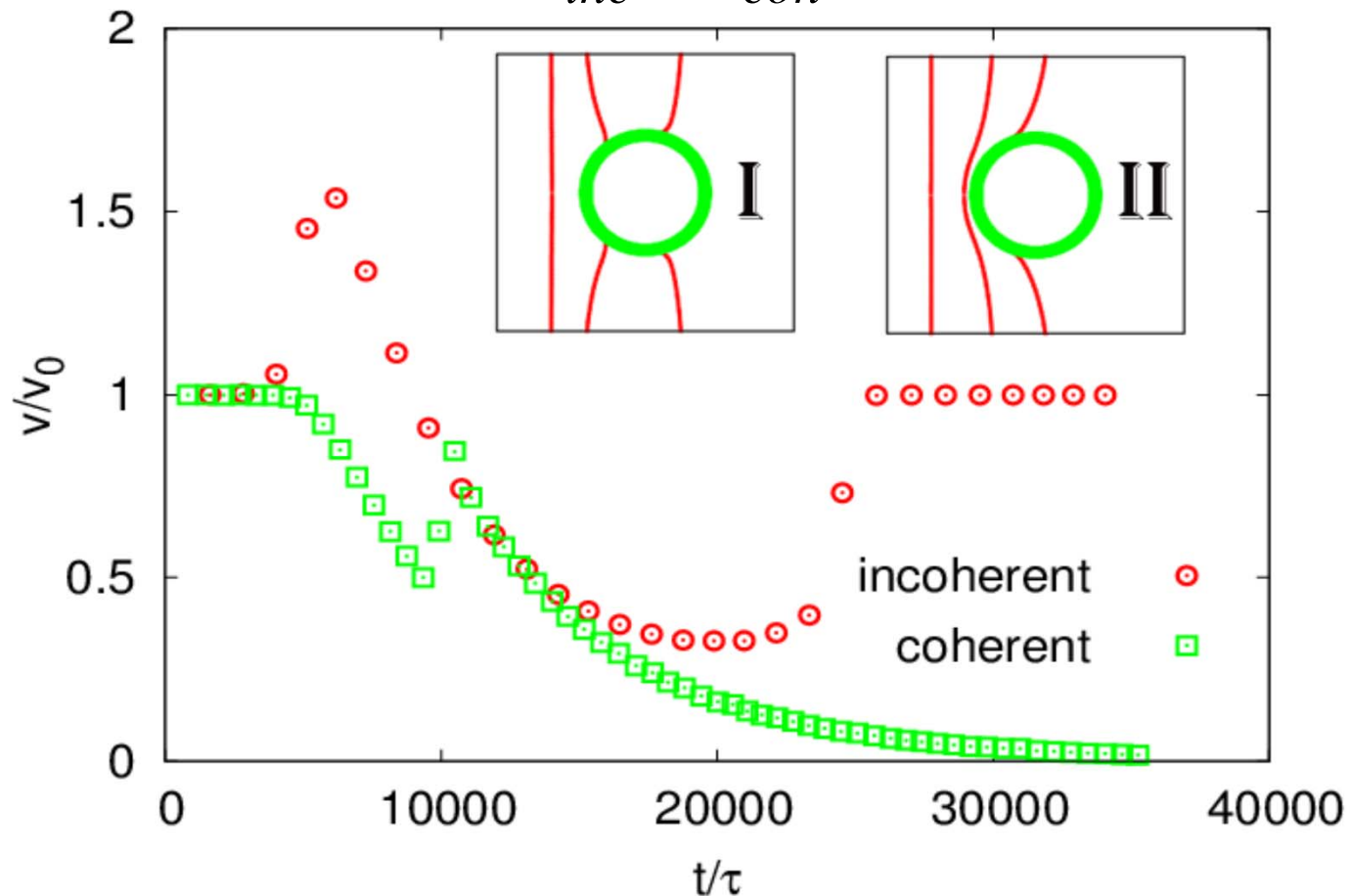


Ellipsoid particles



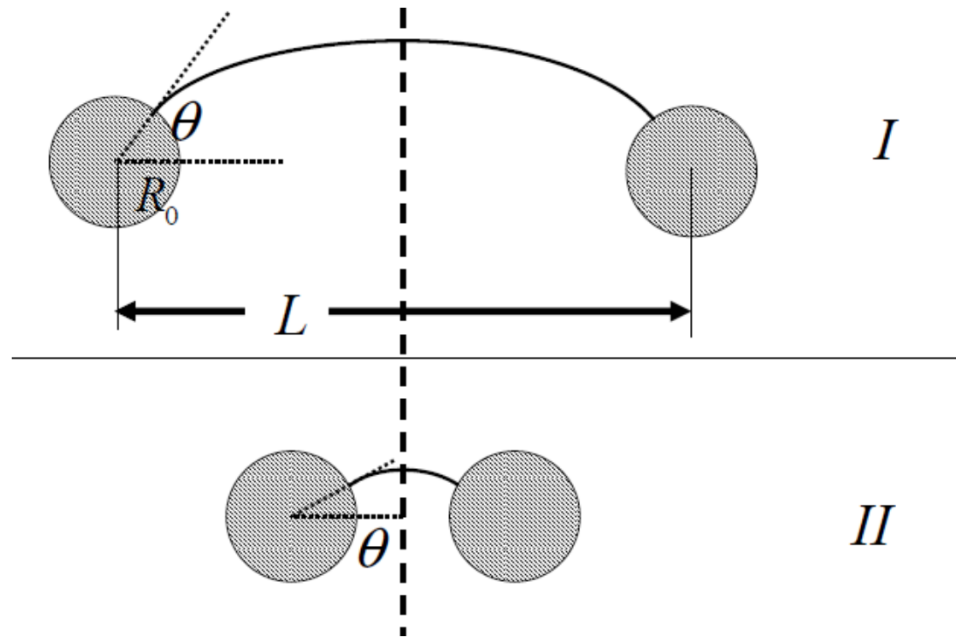
# Phase-field Simulated GB Migration Behavior (Incoherent & Coherent Interfaces)

$$\gamma_{inc} / \gamma_{coh} \geq 5$$



“Pinning force of grain boundary migration from a coherent particle,”  
N. Wang, Y.H. Wen, and L.Q. Chen, Philosophical Magazine Letter, under review

# Particle Spacing (Volume Fraction) Effect



Well separated:

$$L \gg 2R$$

$$\theta^{\max} = \pi / 4$$

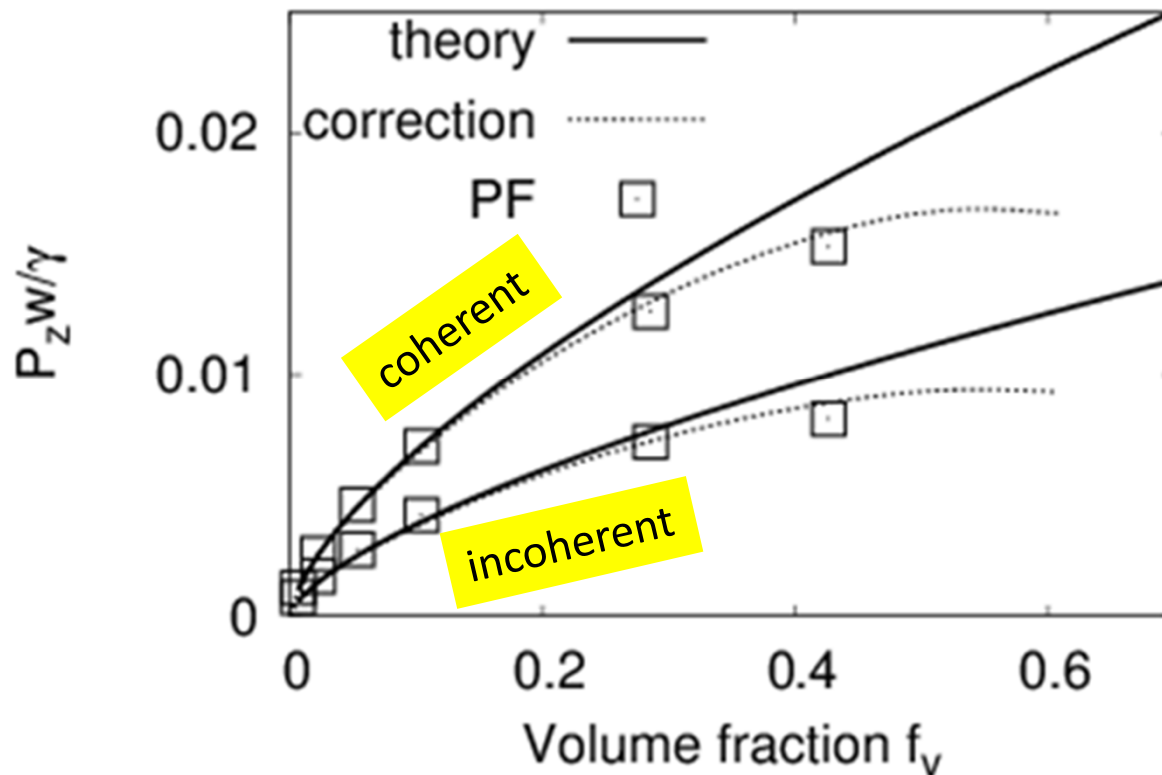
Close neighbor:

$$L \sim 2R$$

$$\theta^{\max} < \pi / 4$$

Cannot reach maximum pinning angle  
due to the constraint of inter-particle surface shape  
An analytical correction term is derived for the 2D case

# Pinning Force Correction at High Volume



Correction to current pinning force theory at high volume fraction validated against PF simulation

“Pinning force from multiple second-phase particles in grain growth,”  
N. Wang, Y.H. Wen, and L.Q. Chen, Computational Materials Science, under review

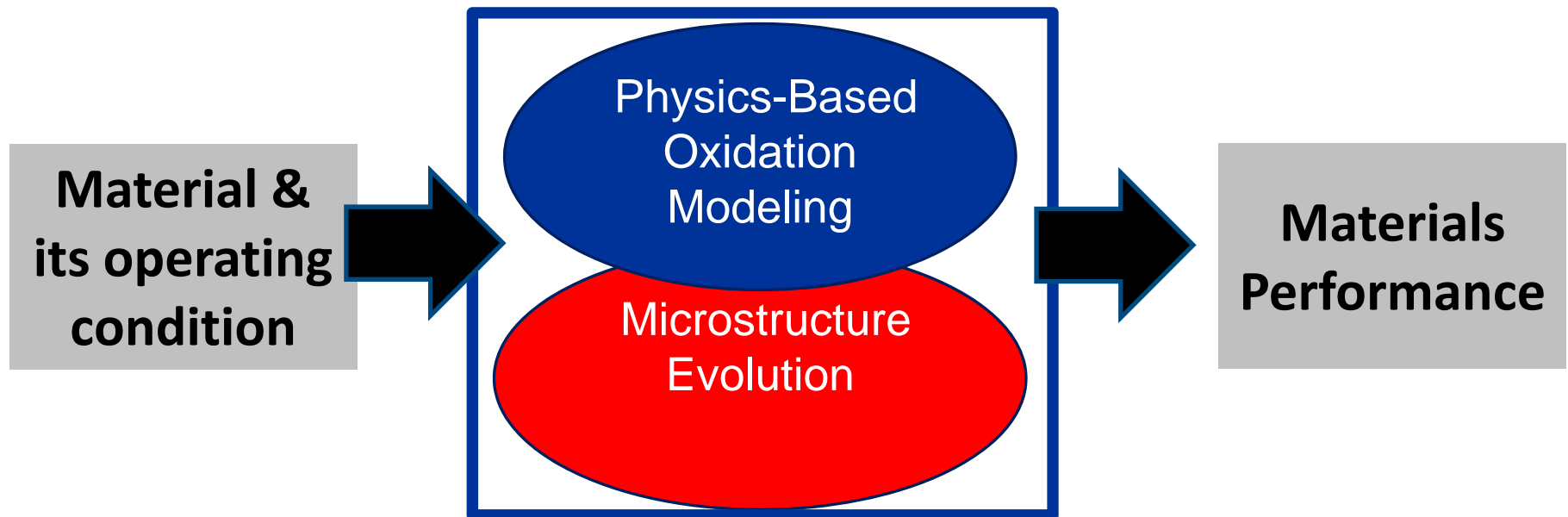
# Summary of 2<sup>nd</sup> Phase Pinning Modeling

- **Developed a first quantitative evaluation for coherent particle pinning force for an ellipsoid particle**
- **Proposed a large volume fraction pinning force correction and verified via Phase-field simulations**

# Metal Oxidation Modeling

## The Goal

Develop a modeling toolbox to link material's operating environment to its performance

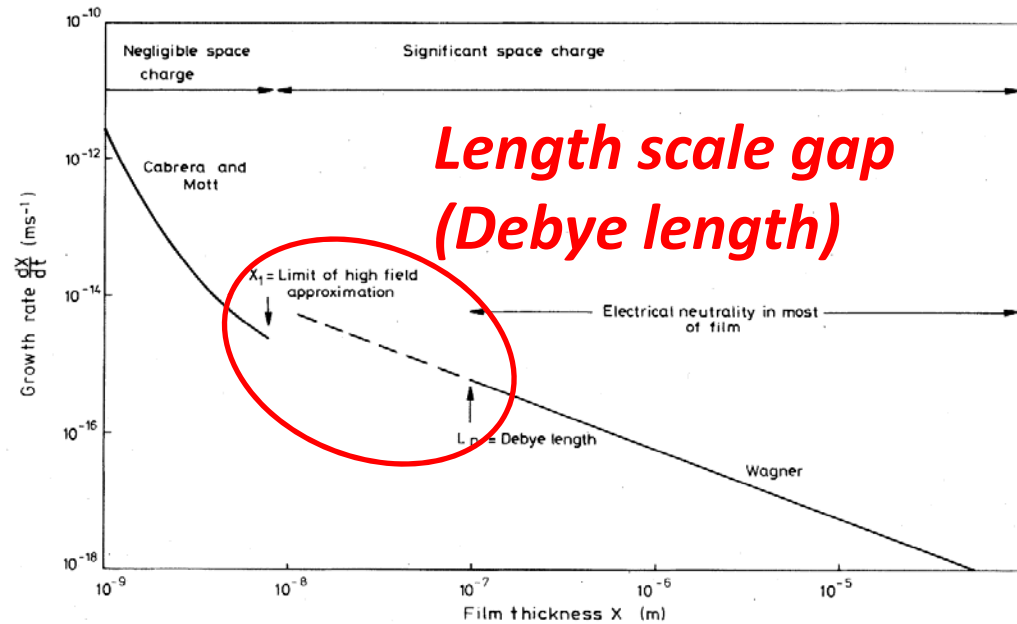


# Metal Oxidation Modeling

Cabrera  
-Mott  
Theory

*Moderate  
film thickness*

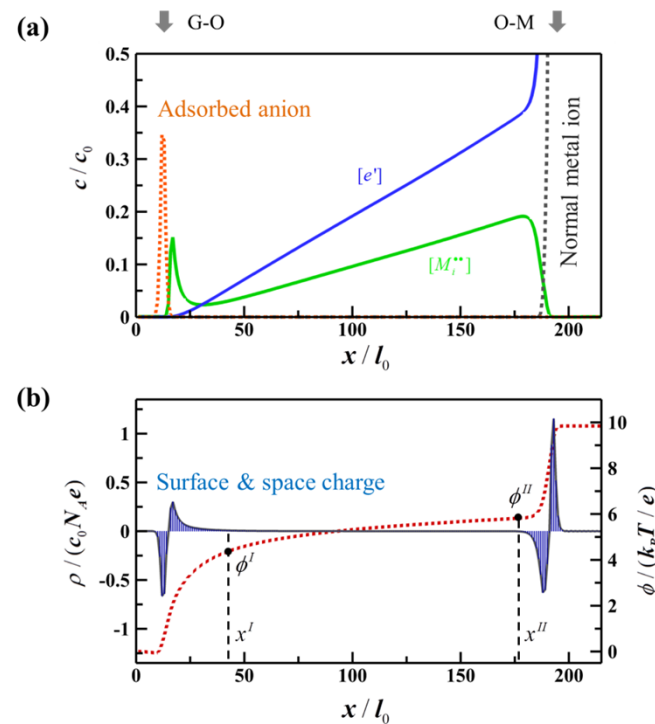
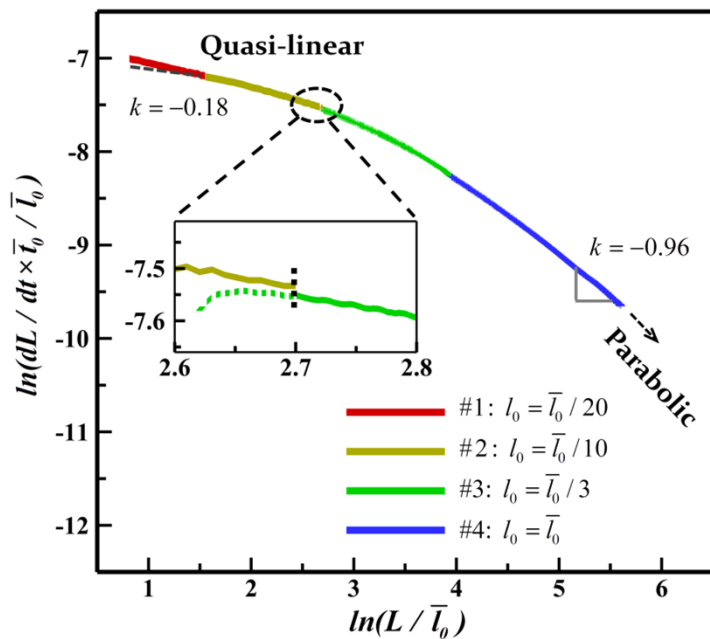
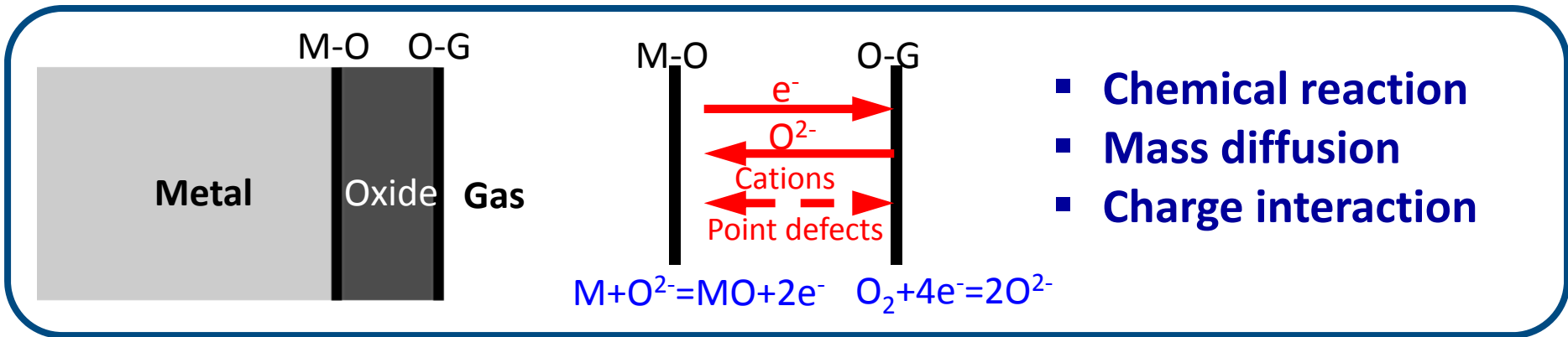
Wagner  
Theory



(Atkinson, *Review of Modern Physics*, 1985)

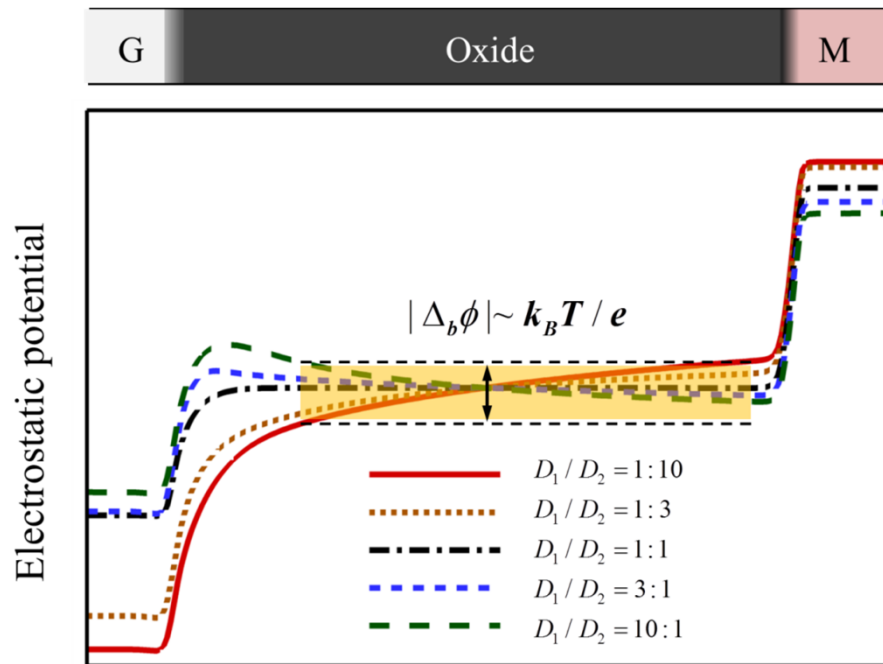
***Moderate film thickness regime:***  
*The coupling of charge interaction, ionic diffusion, and chemical reaction has to be addressed.*

# Progress on Oxidation Kinetics Modeling



T Cheng, Y Wen, J Hawk, J. Phys. Chem. C, 118 (2) (2014) 1269-1284.

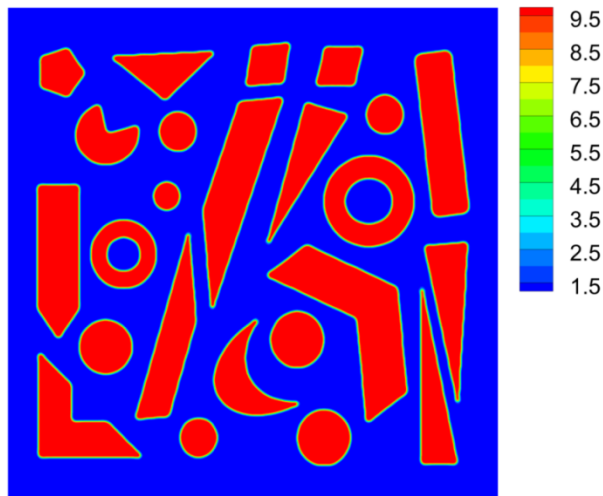
# Electrostatic potential distribution in a growing oxide film under different ion/electron mobility ratios



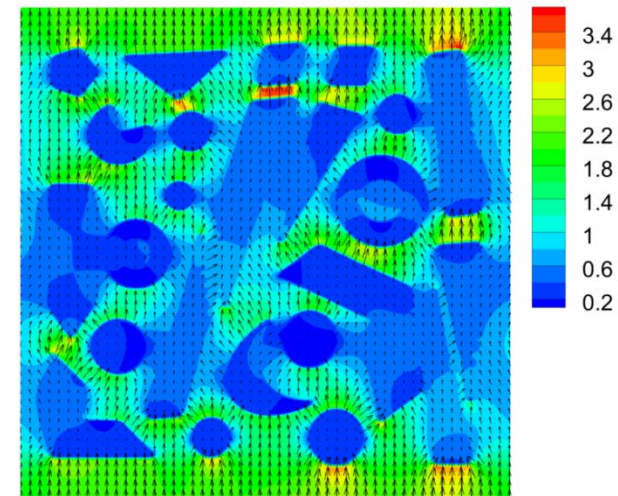
- Developed an analytical model for the electric field in the growing oxide for a simpler prototype oxidation reaction
- Verified via comprehensive phase-field modeling for more sophisticated cases.
- Revealed the electrostatic potential drop across the bulk oxide is limited to  $\sim k_B T / e$

T Cheng, Y Wen, J. Phys. Chem. Letter, under review

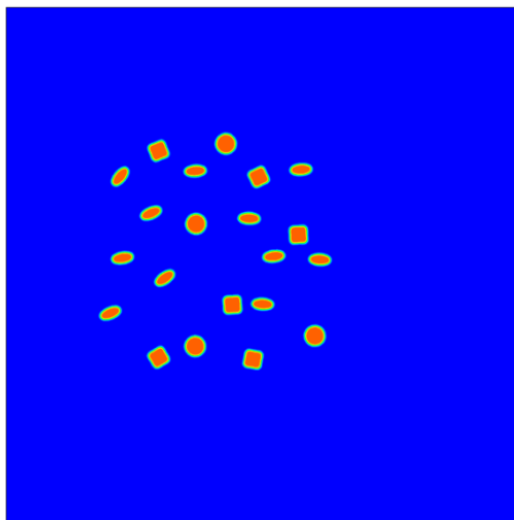
# Efficient Algorithm to Solve Electrostatic Problems



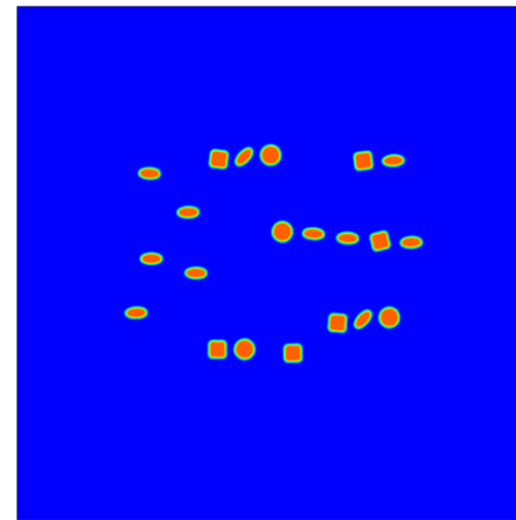
Dielectric constant distribution



Actual electric field distribution



Nonuniform  
external field

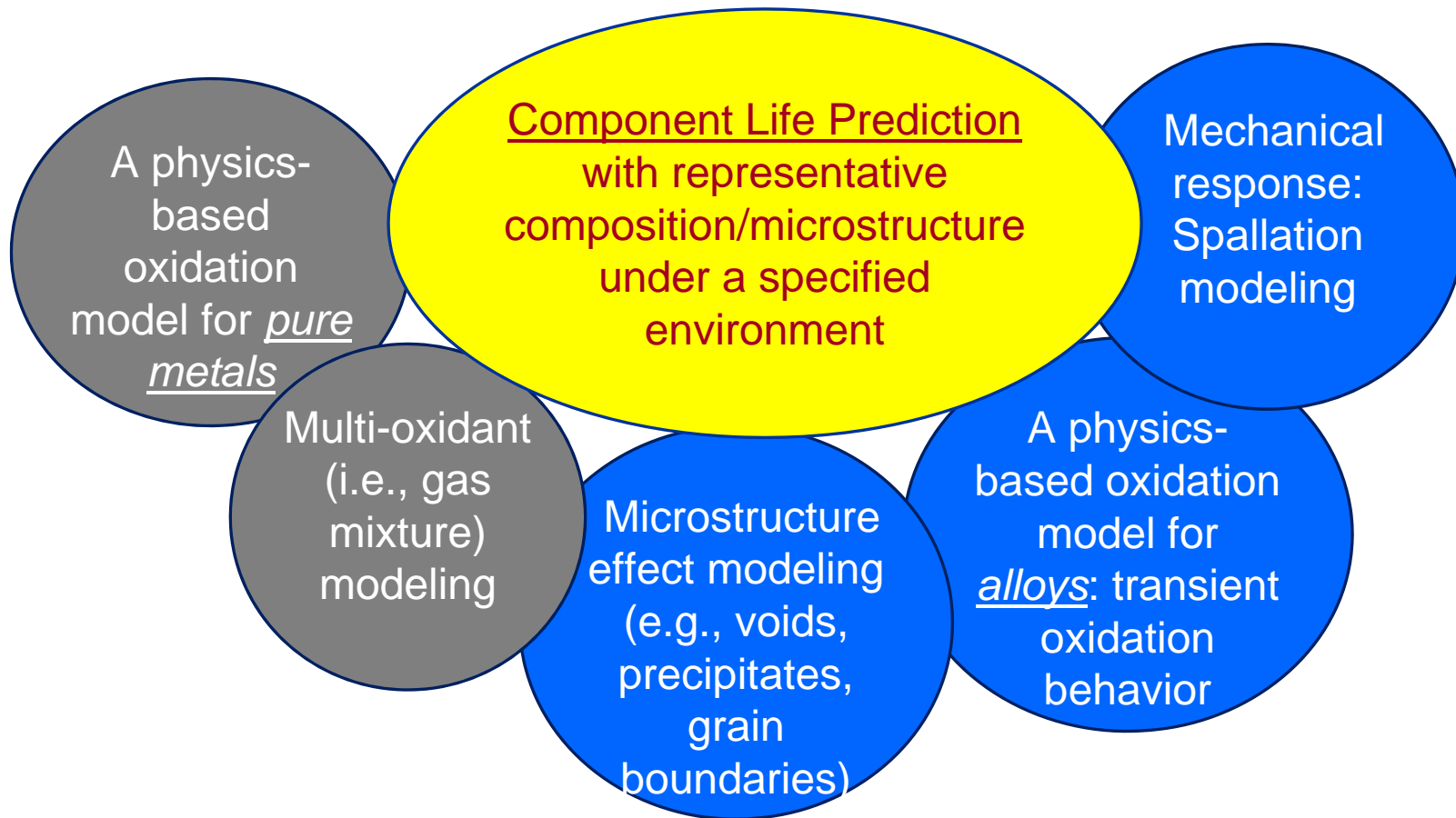


**Dielectrophoresis process with various inter-particle force and hydrodynamic effects**

# Summary of Oxidation Kinetics Modeling

- Developed a *multiscale simulation capability* based on Phase-Field Method to solve the complex coupling problem that involves transport of charged ions subject to interfacial reactions and long range electrostatic interactions
- Developed an *efficient numerical algorithm* to solve the charge interaction problem with arbitrary heterogeneity in electric properties
- Further development of the model is necessary to advance this model into a useful tool that can be used to predict the life of a complex alloy

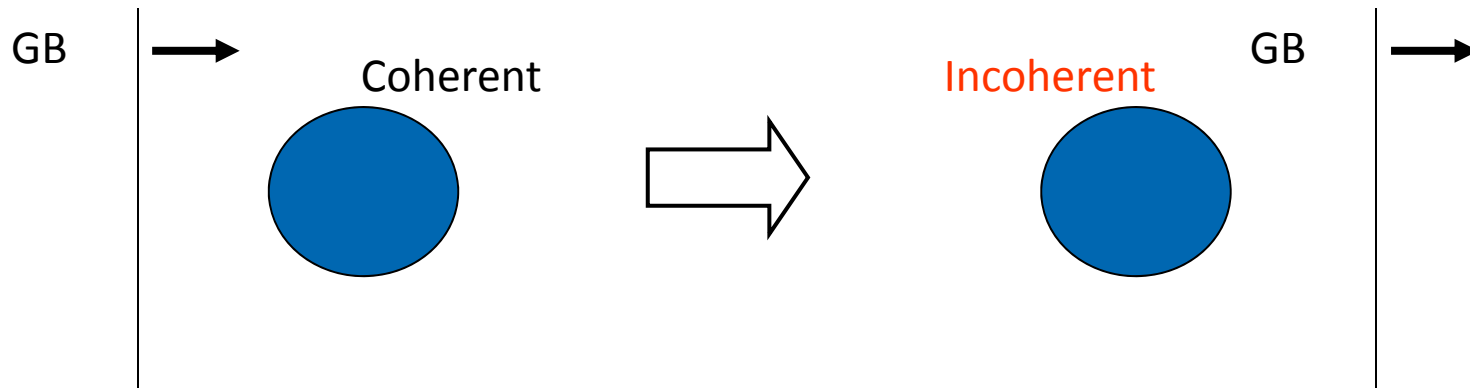
# Roadmap to Oxidation Modeling



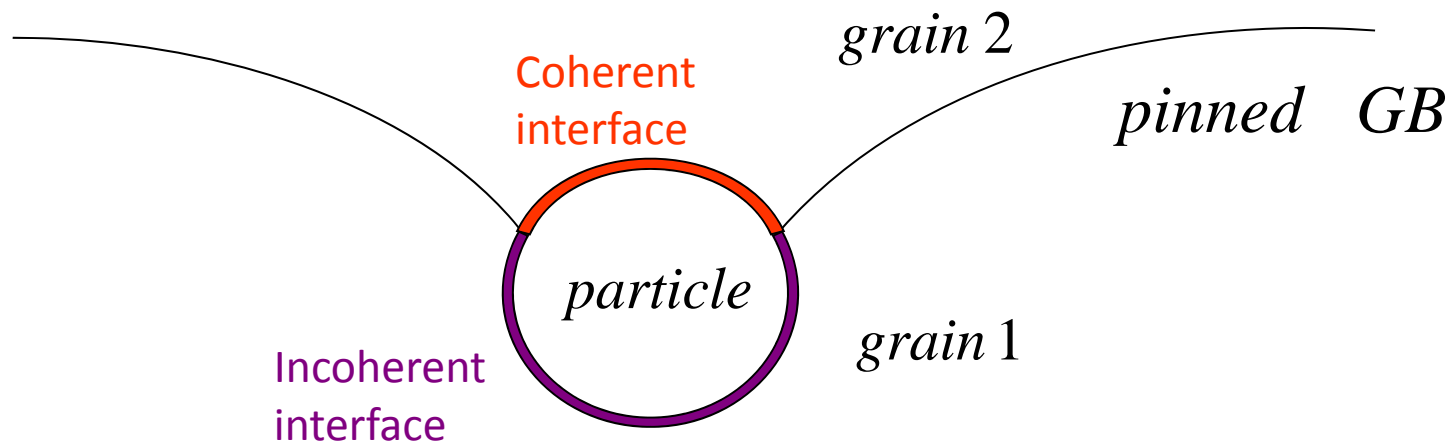
# Backup Slides

# Lattice Coherency of Pinning Particles

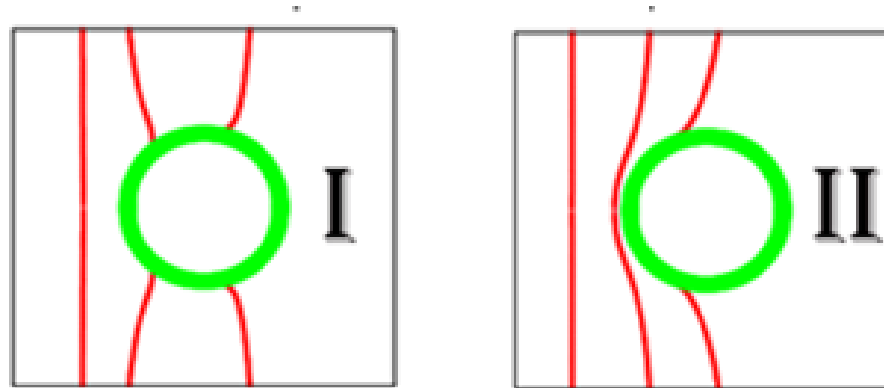
Coherency loss



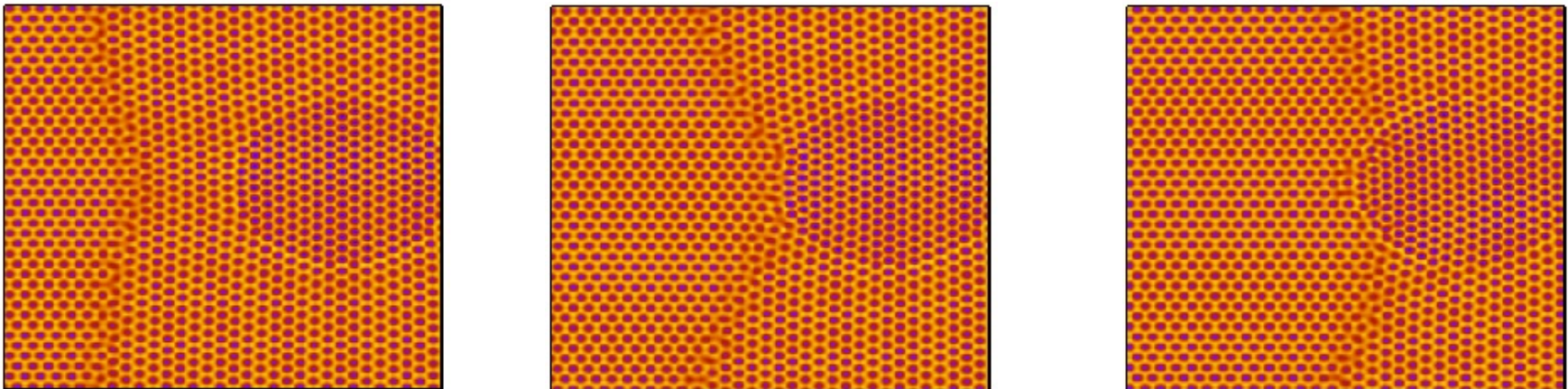
$$\text{Surface energy} \sim \gamma_{inc} / \gamma_{coh} \geq 5 \quad \gamma_{gb} \sim \gamma_{inc}$$



# PFC Results of Coherent Particle Pinning



Interaction between grain boundary and pinning particle under the influence of interfacial energy only ; Incoherent (left) and coherent (right)



GB shape near a coherent particle with large lattice misfit

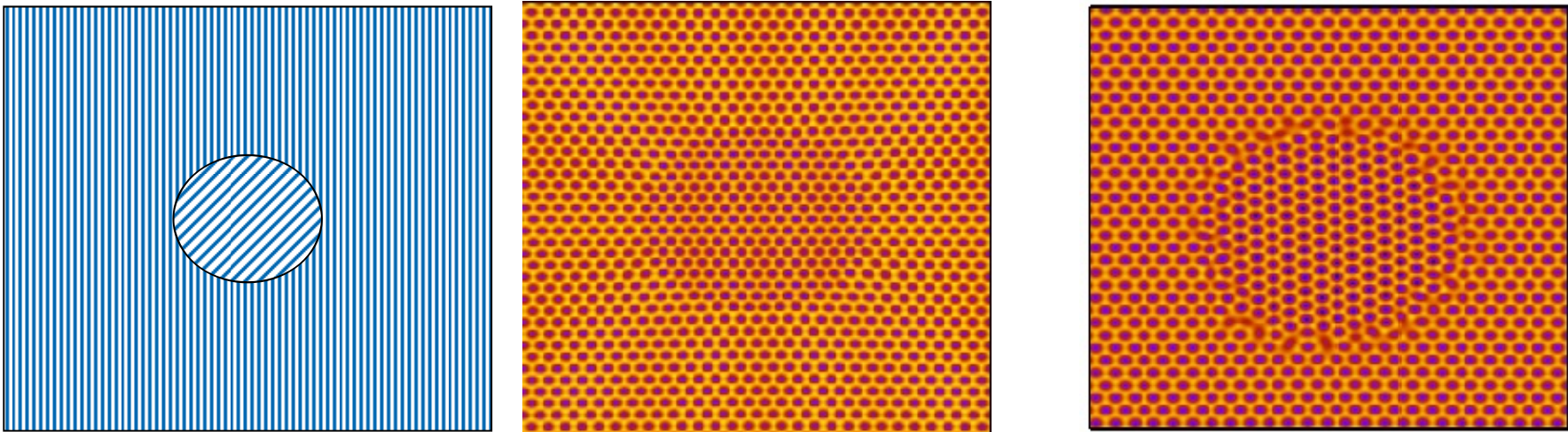
# Lattice Misfit Effect on Particle Pinning

## Phase-Field-Crystal (PFC) Modeling

$$F_{pfc} = \int \left\{ \frac{\varphi}{2} \left[ -\varepsilon + (q^2 + \nabla^2)^2 \right] \varphi + \frac{\varphi^4}{4} \right\} dv$$

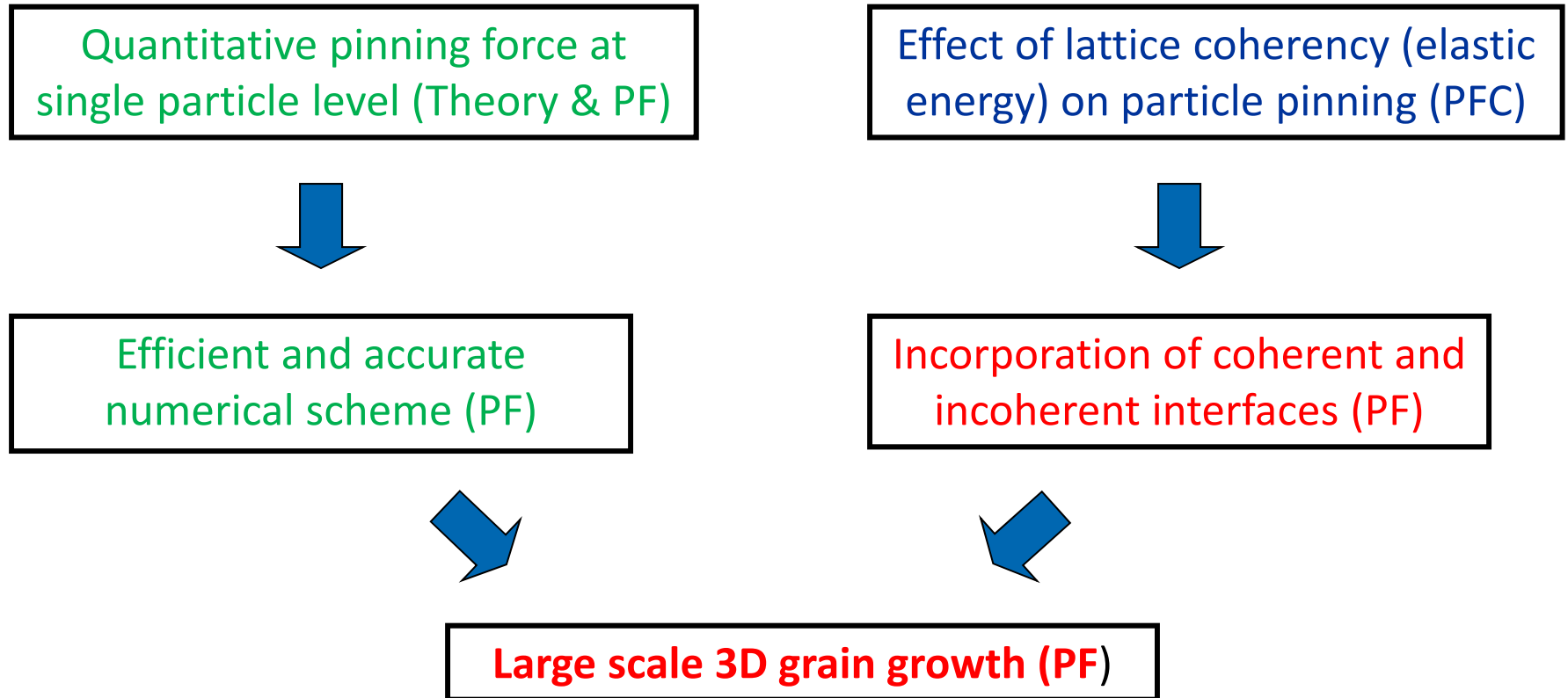
$\varphi$  – atomic density field;  $q$  is related to the lattice parameter

Atomic resolution with intrinsic elasticity and defects evolution;  
ideal for modeling misfit strain effect on particle pinning



Coherency loss with increasing lattice misfit in PFC

# Roadmap to Particle Pinning Modeling



Goal: Quantitative understanding of particle pinning in grain growth

# Multi-Component Multi-Phase Phase-Field Model

## Multi-Component, Multi-Phase

$$F(c, \eta) = \int_{\Omega} [f(c, \eta) + f^{grad} + \dots] d\Omega$$

### Kim-Kim-Suzuki(KKS) Model\*

$$f(c, \eta) = \sum_{i=1}^m \eta_i g^i(c) \quad \text{Link to CALPHAD Database}$$

✓ flexible interfacial energy

✓ practical length scale

$$c_k = \sum_{i=1}^m \eta_i c_k^i \quad \text{Mass Conservation}$$

$$\frac{\partial g^i}{\partial c_k} = \frac{\partial g^j}{\partial c_k} \quad \text{Equal Chemical Potential}$$

### Multiphase Model\*\*

✓ multiphase

✓ multi-variant

✓ poly-crystal

$$f(\eta) + \sum_{i=1}^m \sum_{j>i}^m \omega_{ij} \eta_i^2 \eta_j^2 \quad \text{Local Free Energy Barrier}$$

$$f^{grad} = \sum_{i=1}^m \sum_{j>i}^m \frac{\epsilon_{ij}}{2} (\eta_j \nabla \eta_i - \eta_i \nabla \eta_j)^2 \quad \text{Gradient Energy}$$

\* Kim et al., Phys. Review E, 60(6), 7186(1999)

\*\* Steinbach et al., Physica D, 94, 135(1996)

# Phase-Field Model: (cont.)

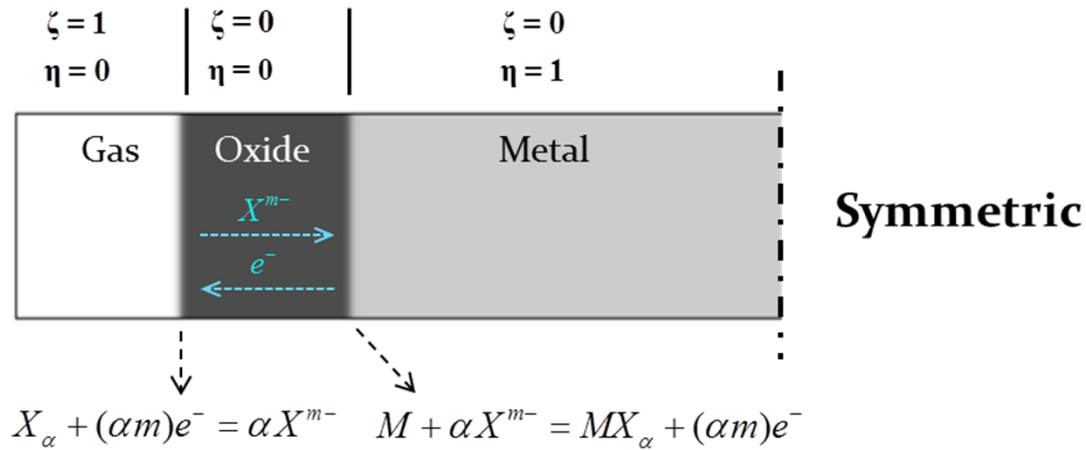
## Elastic Effect due to Lattice Misfit

$$\varepsilon_{ij}^{00}(m) = \delta_{ij} \varepsilon_m^{00} = \delta_{ij} \left[ \frac{\partial a(X)}{a_o \partial X_m} \right] \quad \text{Vegard's law}$$

$$\varepsilon_{ij}^{00}(\vec{r}) = \sum_{m=1}^n \varepsilon_{ij}^{00}(m) X_m(\vec{r}) \quad \text{Composition-dependent eigenstrain}$$

$$F_{el} = \frac{1}{2} \int \frac{d^3 \mathbf{g}}{(2\pi)^3} \left[ C_{ijkl} \{ \varepsilon_{ij}^0(\mathbf{r}) \}_{\mathbf{g}} \{ \varepsilon_{kl}^0(\mathbf{r}) \}_{\mathbf{g}}^* - n_i \{ \sigma_{ij}^0(\mathbf{r}) \}_{\mathbf{g}} \Omega_{jk}(\mathbf{n}) \{ \sigma_{kl}^0(\mathbf{r}) \}_{\mathbf{g}}^* n_l \right]$$

# Oxidation Model Description



$$\frac{d[X^-]}{dt} = k_I p_X ([X^-]^* - [X^-])[e^-] \qquad \frac{d[X^-]}{dt} = \frac{d[M]}{dt} = -k_{II}[M][X^-]$$

$$\frac{d[e^-]}{dt} = -k_I p_X ([X^-]^* - [X^-])[e^-] \qquad \frac{d[e^-]}{dt} = k_{II}[M][X^-]$$

(cf. Standard Deal-Grove oxidation model)

**Boundary condition:**

**Metal phase:** electric field inside a conductor should be zero.

(large mobility electrons + background cations)

**Gas phase:** Diffusing species are prohibited to enter

# Governing Equations

	Reaction	Diffusion + Electromigration
[X <sup>-</sup> ]:	$\frac{\partial c_1}{\partial t} = K_I p_X \Lambda_\xi c_2 (\bar{c}_1 - \tilde{c}_1) - K_{II} \Lambda_\eta \tilde{c}_1$	$+ \nabla \cdot (D_1 \nabla c_1) - \frac{e}{k_B T} \nabla \cdot (D_1 c_1 z_1 \mathbf{E})$
[e <sup>-</sup> ]:	$\frac{\partial c_2}{\partial t} = -K_I p_X \Lambda_\xi c_2 (\bar{c}_1 - \tilde{c}_1) + K_{II} \Lambda_\eta \tilde{c}_1$	$+ \nabla \cdot (D_2 \nabla c_2) - \frac{e}{k_B T} \nabla \cdot (D_2 c_2 z_2 \mathbf{E})$
[c <sup>+</sup> ]:	$\frac{\partial c_3}{\partial t} =$	$\nabla \cdot (D_3 \nabla c_3) - \frac{e}{k_B T} \nabla \cdot (D_3 c_3 z_3 \mathbf{E})$
[M]:	$\frac{\partial \eta}{\partial t} = -K_V K_{II} \Lambda_\eta \tilde{c}_1$	$+ M_\eta \nabla^2 (\partial f / \partial \eta - \beta \nabla^2 \eta)$

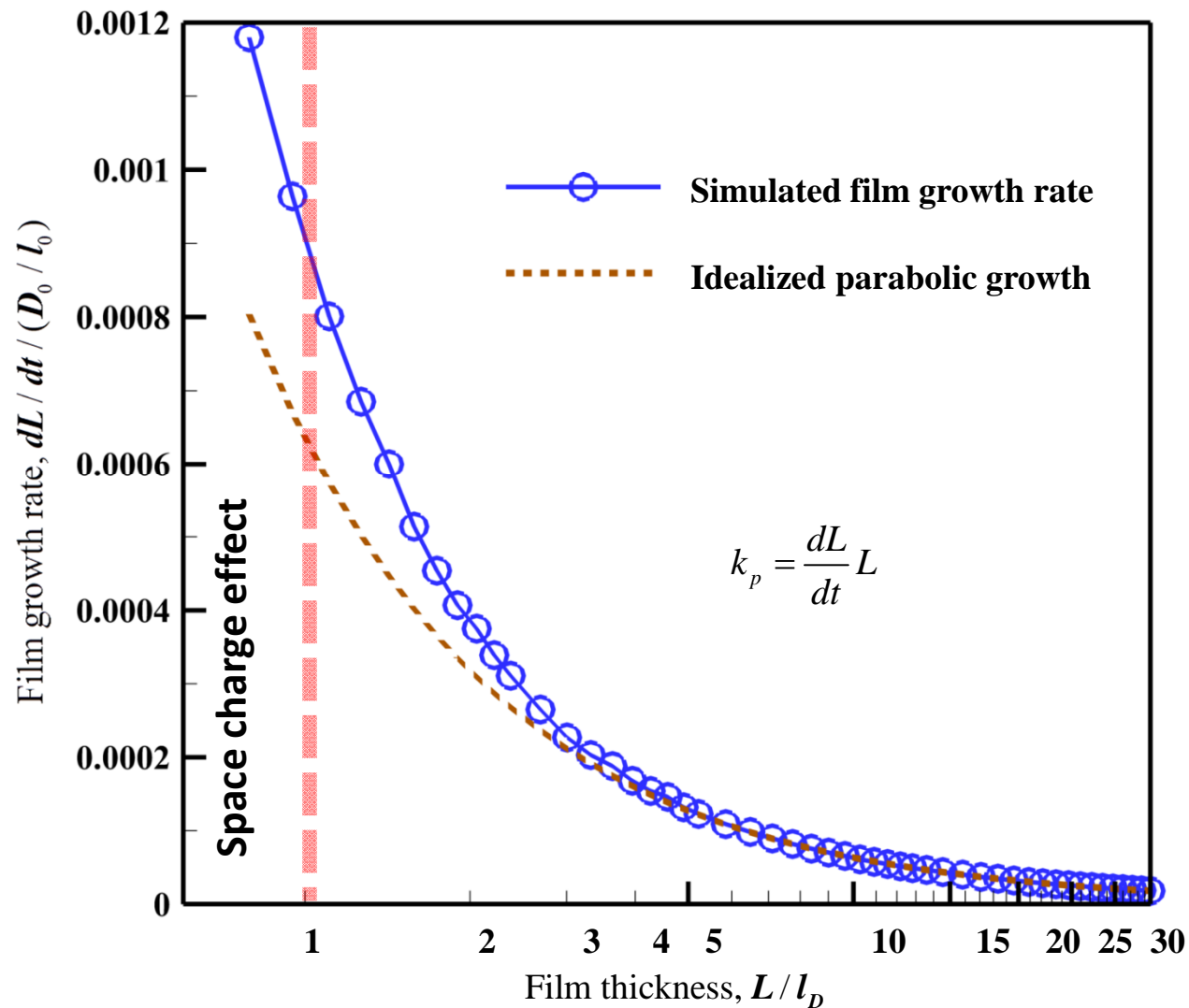
$$\tilde{c}_i = (1 + \kappa_G \zeta + \kappa_M^{(i)} \eta) c_i$$

$$\Lambda_\eta = \eta^p (1 - \eta)^q, \quad \Lambda_\xi = \xi^p (1 - \xi)^q$$

$$F(\eta) = \int \left[ f(\eta) + \frac{1}{2} \beta |\nabla \eta|^2 \right] dV$$

The electric field, satisfying Poisson's equation, is solved by an **efficient numerical scheme** for arbitrary **dielectric heterogeneity**

# Simulated Kinetics vs Wagner Theory



**Parabolic growth at the thick film stage and the deviation by the space charge effect when the film thickness is approaching the Debye length**